AD_____

Molecular Basis of Paralytic Neurotoxin Action on Voltage-Sensitive Sodium Channels

Annual Report

William A. Catterall, Ph.D.
Professor and Chairman
Department of Pharmacology

October 20, 1987

Supported by

U.S. ARMY MEDICAL RESEARCH AND DEVELOPMENT COMMAND
Fort Detrick, Frederick, Maryland 21701-5012

Contract No. DAMD17-84-C-4130

University of Washington
Seattle, Washington 98195

Approved for public release; distribution unlimited

AD-A191264

SECURITY CLASSIFICATION OF THIS PAGE

REPORT DOCUMENTATION PAGE

Form Approved
OMB No 0704-0188
Exp Date Jun 30 1986

1a REPORT SECURITY CLASSIFICATION: Unclassified	1b RESTRICTIVE MARKINGS
2a SECURITY CLASSIFICATION AUTHORITY	3 DISTRIBUTION/AVAILABILITY OF REPORT: Approved for public release; distribution unlimited
2b DECLASSIFICATION/DOWNGRADING SCHEDULE	
4 PERFORMING ORGANIZATION REPORT NUMBER(S)	5 MONITORING ORGANIZATIO... ...T NUMBER(S)
6a NAME OF PERFORMING ORGANIZATION: University of Washington; 6b OFFICE SYMBOL (If applicable)	7a NAME OF MONITORING ORGANIZATION
6c. ADDRESS (City, State, and ZIP Code): Department of Pharmacology, Seattle, Washington 98195	7b. ADDRESS (City, State, and ZIP Code)
8a. NAME OF FUNDING/SPONSORING ORGANIZATION: U.S. Army Medical Research & Development Command; 8b OFFICE SYMBOL (If applicable)	9. PROCUREMENT INSTRUMENT IDENTIFICATION NUMBER: DAMD17-84-C-4130
8c. ADDRESS (City, State, and ZIP Code): Fort Detrick, Frederick, MD 21701-5012	10. SOURCE OF FUNDING NUMBERS: PROGRAM ELEMENT NO. 61102A; PROJECT NO. 3M161... 102BS12; TASK NO. AA; WORK UNIT ACCESSION NO 111

11. TITLE (Include Security Classification)
(U) Molecular Basis of Paralytic Neurotoxin Action on Voltage-Sensitive Sodium Channels

12. PERSONAL AUTHOR(S)
William A. Catterall, Ph.D.

13a. TYPE OF REPORT	13b. TIME COVERED	14. DATE OF REPORT (Year, Month, Day)	15. PAGE COUNT
Annual Report	FROM 9/15/86 TO 9/14/87	1987, October 20	50

16. SUPPLEMENTARY NOTATION

17. COSATI CODES			18. SUBJECT TERMS (Continue on reverse if necessary and identify by block number)
FIELD	GROUP	SUB-GROUP	Ion transport, sodium channels, action potentials, electrical excitability, neurotoxins
06	01		
06	15		

19. ABSTRACT (Continue on reverse if necessary and identify by block number)

In years 1 - 3 of this project, progress was made on several objectives:

A. The sites and mechanisms of action on the sodium channel were examined and further defined for three new classes of neurotoxins: Goniopora toxins, Brevetoxins, and Conotoxins.

B. Monoclonal antibodies with high affinity for the mammalian neuronal sodium channe were developed and methods to screen them for activity at neurotoxin binding site were established.

C. Site-directed antibodies against defined regions of the amino acid sequence of th sodium channel were prepared and shown to bind at discrete negatively charged subsites on the extracellular surface of the channel that may form part of neurotoxin receptor sites.

20 DISTRIBUTION/AVAILABILITY OF ABSTRACT	21 ABSTRACT SECURITY CLASSIFICATION
☒ UNCLASSIFIED/UNLIMITED ☐ SAME AS RPT ☐ DTIC USERS	
22a NAME OF RESPONSIBLE INDIVIDUAL: Mrs. Judy Pawlus; 22b TELEPHONE (Include Area Code): 301-663-7325; 22c OFFICE SYMBOL: SGRD-RMI-S	

DD FORM 1473, 84 MAR — 83 APR edition may be used until exhausted. All other editions are obsolete.

SECURITY CLASSIFICATION OF THIS P...

TABLE OF CONTENTS

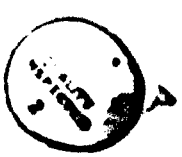

Foreword

In conducting this research described in this report, the investigator(s) adhered to the "Guide for the Care and Use of Laboratory Animals," prepared by the Committee on Care and use of Laboratory Animals of the Institute of Laboratory Animal Resources. National Research Council (DHEW Publication No. (NIH) 86-23, Revised 1985).

RESEARCH REPORT

In the third year of this project, we have continued to analyze the effects of newly described neurotoxins on voltage sensitive sodium channels in mammalian neurons, prepared site-directed antisera against several defined segments of the sodium channel and used these to probe the structure, function, and distribution of neurotoxin receptor sites on sodium channels.

A. Neurotoxin Action on Sodium Channels

1. Site and Mechanism of Action of Conotoxin Toxin

The results on the site and mechanism of action of Conotoxin toxin on sodium channels described in our previous Annual Report (October 14, 1985) have been published in *Molecular Pharmacology* (Gonoi et al., 1986).

2. Site of Inhibition of Sodium Channels by μ Conotoxins

The results on the site of action of μ-conotoxins described in last year's Annual Report (October 14, 1986) have now been published in the *Journal of Biological Chemistry* (Ohizumi, et al., 1986).

3. Inhibition of Tetrodotoxin-sensitive and -insensitive Sodium Channels by μ Conotoxins

Two pharmacologically distinct subtypes of voltage-sensitive sodium channels have been described in mammalian muscle cells. The TTX-sensitive sodium channels of adult muscle are blocked by tetrodotoxin binding at neurotoxin receptor site 1 with an apparent K_D of approximately 10 - 20 nM (reviewed by Ritchie and Rogart, 1977). Denervation of adult muscle causes appearance of TTX-insensitive sodium channels with apparent K_D values of approximately 1 μM for tetrodotoxin (Harris and Thesleff, 1971; Pappone, 1980). TTX-insensitive sodium channels are also present in fetal rat muscle developing *in vivo* (Harris and Marshall, 1973). Dissociated cultures of rat muscle cells developing *in vitro* express both TTX-insensitive sodium channels (Kidokoro et al, 1975; Catterall, 1976; Sastre and Podleski, 1976; Stallcup and Cohn, 1976) and TTX-sensitive sodium channels (Sherman et al, 1983; Frelin et al, 1983) which function in parallel as assessed by ion flux (Sherman et al, 1983), voltage clamp (Gonoi et al, 1985), and single channel recording (Weiss et al, 1986) methods.

Venom of the marine snail *Conus geographus* contains polypeptide toxins of novel structure (Nakamura et al, 1983; Sato et al, 1983; Cruz et al, 1985) which inhibit skeletal muscle contraction (Nakamura et al, 1983) by preferentially blocking muscle sodium channels (Minoshima et al, 1984; Cruz et al, 1985). Sodium channels in neuronal preparations are not blocked at similar toxin concentrations (Cruz et al, 1985; Ohizumi et al, 1986a). Geographutoxin II (GTX II), the most potent of this family of conotoxins, competitively inhibits binding of [^{3}H] saxitoxin to neurotoxin receptor site 1 on muscle sodium channels at concentrations similar to those that inhibit sodium channel function (Ohizumi et al, 1986b; Moczydlowski et al, 1986; Yanagawa et al, 1986). Saxitoxin binding to sodium channels in synaptosomes or superior cervical ganglion is unaffected at similar concentrations. Since saxitoxin and TTX bind similarly to sodium channels of nerve and adult skeletal muscle, GTX II is the first ligand that distinguishes between the structures of neurotoxin receptor 1 on sodium channels in these tissues. This toxin may therefore provide the most sensitive probe of structural differences in this site on sodium channel subtypes. In these experiments, we have examined the action of this toxin on

TTX-sensitive and TTX-insensitive sodium channels in spherical myoballs (Fukuda et al, 1976) prepared from cultured rat muscle cells developing in vitro using the giga ohm seal, whole cell voltage clamp procedure of Hamill et al (1981) as described previously (Gonoi et al, 1985).

The primary structure of GTX II is illustrated in Figure 1. It is a 22 residue polypeptide containing 3 hydroxyproline residues, three positively charged arginine residues, and three disulfide bonds (Sato et al, 1983). The guanidine moieties of two of the arginine residues are likely to occupy similar positions in neurotoxin receptor site 1 of the sodium channel to the guanidine moieties of tetrodotoxin and saxitoxin. The larger size of GTX II may provide other points of attachment which result in selective binding to sodium channel subtypes.

Rat muscle cells were dissociated from embryonic limb muscles and myoballs were prepared. A giga-ohm seal was formed on an individual myoball and sodium currents were recorded over approximately 10 min while the intracellular solution exchanged with the pipette solution and the amplitude of sodium currents reached steady state. A family of sodium current responses elicited by depolarization to membrane potentials of -90 mV to +60 mV before toxin treatment is illustrated in Figure 2A. The sodium channel density and the kinetic and voltage-dependent parameters describing these sodium currents agreed closely with those measured previously (Gonoi et al, 1985). Addition of GTX II to a final concentration of 2.5 μM in the recording medium caused a progressive reduction in the sodium current recorded at a pulse potential of -20 mV. The sodium current reached a new steady state after approximately 2 min (Figure 2B). Neither the time course nor the voltage-dependence of the remaining sodium current was altered markedly by toxin treatment (Figure 2C).

Cumulative addition of GTX II to individual myoballs under voltage clamp caused progressive reduction in peak sodium conductance as illustrated for two representative myoballs in Figure 3. After each addition, sodium conductance declined to a new steady state within 5 min. Currents were recorded within 10 min after each addition. For the two myoballs illustrated, 61% and 35% of the sodium conductance was inhibited at a maximum concentration of GTX II. Concentration-effect curves, calculated by least squares analysis assuming noncooperative one-to-one binding of GTX II to 61% and 35% of the sodium channels, respectively, fit the data closely and yield apparent K_D values 21 nM and 27 nM for GTX II action on these two myoballs. These apparent K_D values agree closely with those for block of contraction, sodium currents, and [^{3}H] saxitoxin binding in adult muscle (Nakamura et al, 1983; Cruz et al, 1985; Ohizumi et al, 1986) and therefore represent inhibition of TTX-sensitive sodium channels in the rat muscle cells.

In order to analyze the mean properties of a larger number of myoballs, four myoballs in different petri dishes were studied at each GTX II concentration and mean values of the ratio of sodium conductance in the presence and absence of GTX II were determined. Figure 4 illustrates the measured sodium conductance as a function of GTX II concentration. Analysis of these data as described above showed that 49 $\pm$ 9% of the sodium conductance was inhibited with an apparent K_D of 10 nM in agreement with the data from studies of individual myoballs.

These results show that individual myoballs contain two classes of sodium channels with respect to inhibition by GTX II. The sodium channels that are inhibited by GTX II have the same affinity for GTX II as the TTX-sensitive sodium channels in adult muscle. If TTX-sensitive sodium channels are preferentially inhibited by GTX II, the sodium channels remaining active in the presence of a saturating concentration of GTX II

should all be the TTX-insensitive subtype. Figure 5 illustrates a concentration-effect curve for inhibition by TTX of the sodium conductance that remains in the presence of 2.5 μM GTX II. In the cell cultures used for this experiment, 2.5 μM GTX II reduced sodium conductance to 55.8 ± 8.4% (S.E.M., n = 6) of control values. The sodium conductance that remained was unaffected by 25 nM TTX indicating that no TTX-sensitive sodium channels remained active in the presence of 2.5 μM GTX II. Figure 5 The remaining sodium conductance was completely inhibited by higher concentrations of TTX with an apparent K[D] value of 1.3 μM, identical to that for block of TTX-sensitive sodium channels (Kidokoro et al, 1975; Catterall, 1976; Sastre and Narleski, 1976; Schmidt and Cohn, 1976; Pappone, 1980; Lawrence and Catterall, 1981; Frelin et al, 1983; Sherman et al, 1983; Gonoi et al, 1985). The concentration effect curve calculated assuming noncooperative, one-to-one binding to a single site fits the data closely. The results show that GTX II completely blocks the TTX-sensitive sodium channels in cultured rat muscle cells leaving TTX-insensitive sodium channels unaffected.

Inhibition of TTX-insensitive sodium channels by TTX in heart (Cohen et al, 1981) and skeletal muscle (Gonoi et al, 1985) is frequency-dependent while inhibition of TTX-sensitive channels is not. We examined whether repetitive depolarization enhances block of sodium channels in myoballs by GTX II by stimulating with a train of 20 test pulses from a holding potential of -120 mV to -20 mV for 10 msec at a frequency of 0.5, 1, or 2 Hz. Similar conditions cause frequency-dependent block of TTX-insensitive sodium channels in myoballs by TTX (Gonoi et al, 1985). In the presence of 25 nM, 2.5 μM, or 25 μM GTX II, no enhancement of sodium channel inhibition by repetitive stimulation was observed. Thus, repetitive activation of sodium channels does not induce block of TTX-insensitive sodium channels by GTX II and the block of TTX-sensitive sodium channels by this agent is not frequency dependent under these conditions.

Our results further establish GTX II as the most selective ligand for neurotoxin receptor site 1 on the sodium channel. Not only does this toxin distinguish clearly between TTX-sensitive sodium channels in nerve and muscle (Cruz et al, 1985; Ohizumi et al, 1986a), but it also distinguishes more clearly between the TTX-sensitive and -insensitive sodium channels in rat muscle than does TTX itself. TTX binds to TTX-sensitive sodium channels with approximately 200-fold higher affinity than TTX-insensitive sodium channels. GTX II binds to and inhibits TTX-sensitive sodium channels with at least 10,000 fold higher affinity than TTX-insensitive sodium channels (Figure 3 and 4). It may have no action on TTX-insensitive sodium channels at all. These results provide the clearest evidence to date that the TTX-sensitive and -insensitive sodium channels in skeletal muscle are structurally distinct entities. TTX-insensitive sodium channels in skeletal muscle have three additional properties which distinguish them from TTX-sensitive sodium channels. (i) They have higher affinity for Anemonia sulcata sea anemone toxin II than for Leiurus α-scorpion toxin at neurotoxin receptor site 3 (Lawrence and Catterall, 1981a,b; Frelin et al, 1984). (ii) Their inhibition by tetrodotoxin is frequency-dependent (Gonoi et al, 1985). (iii) They have lower single channel conductance and altered voltage-dependence (Weiss et al, 1986). TTX-insensitive sodium channels with similar properties are present in mammalian cardiac cells at all times (Reuter, 1979; Cohen et al, 1981; Catterall and Coppersmith, 1981). Considered together, these observations provide strong evidence that these two classes of sodium channels represent distinct pharmacological subtypes which are differentially expressed in muscle tissues.

The present results also provide the clearest evidence to date that rat muscle cells cultured in vitro in the absence of neurons are able to synthesize functional TTX-sensitive sodium channels characteristic of adult skeletal muscle. In previous studies (Sherman et al, 1983; Gonoi et al, 1985; Weiss and Horn, 1986), the presence of

functional forms of TTX-sensitive and -insensitive sodium channels in cultured muscle cells has been inferred from analysis of biphasic TTX inhibition curves which revealed two components of sodium conductance with apparent K_D values characteristic of these two channel subtypes. In contrast, GTX II gives all-or-none inhibition of these two channel subtypes providing a definitive demonstration of the existence of two functional classes of channels. Evidently, rat muscle cells have the intrinsic capacity to synthesize functional TTX-sensitive sodium channels in the absence of innervation in vivo (Sherman and Catterall, 1982) and in vitro (Sherman et al, 1983; Gonoi et al, 1985; Weiss and Horn, 1986; this report). Innervation, and the electrical activity it stimulates in the muscle cell, regulate the cell surface density of functional channels (Sherman and Catterall, 1982, 1984). GTX II will be a valuable experimental probe in further studies of this regulatory process.

4. Modification of Sodium Channel Inactivation by a Toxin from Conus Striatus

The piscovorous marine snails of the genus Conus produce a variety of polypeptide toxins which are used in the capture of prey (Kobayashi, et al, 1982; Olivera, et al, 1985). The primary structures and mechanisms of action of low molecular weight toxins of 12 to 26 amino acid residues which block nicotinic acetylcholine receptors (Gray, et al, 1981), sodium channels (Sato, et al, 1983; Cruz, et al, 1985), and calcium channels (Olivera, et al, 1985; Olivera, et al, 1984) have been described previously. The μ conotoxins, Geographutoxin I and II, from Conus geographus inhibit muscle sodium channels specifically (Olivera, 1985; Kobayashi, et al, 1986; by binding at the same receptor site as tetrodotoxin and saxitoxin (Ohizumi, et al, 1986; Moczydlowski, et al, 1986; Yanagawa, et al, 1986). The venom of Conus striatus causes contracture of skeletal and smooth muscles (Endean, et al, 1967; Endean, et al, 1977; Kobayashi, et al, 1981), positive inotropic effects in the heart (Endean, et al, 1979; Kobayashi, et al, 1982), and repetitive firing and prolonged action potentials in myelinated nerve (Endean, et al, 1976; Hahin, et al, 1981). A purified glycoprotein with a molecular weight of 25,000 retains the positive inotropic activity of the whole venom suggesting that it is a major toxic component (Kobayashi, et al, 1982). In this report, we describe the actions of this purified protein on sodium currents in mouse neuroblastoma cells and on binding of specific neurotoxins to their sites of action on sodium channels in rat brain synaptosomes.

Modification of sodium channel kinetics by CsTx. Sodium currents mediated by voltage-sensitive sodium channels were measured by the whole cell voltage clamp technique. Fig. 6A illustrates a family of sodium currents elicited by depolarizations to test potentials of -50 mV to +80 mV at intervals of 1 sec. Sodium channels are activated within 1 msec and are inactivated within a few msec depending on the test potentials applied. This recording was made 20 min after making a high resistance seal between the cell membrane and a micropipet. By this time the exchange of ions between the cell and the micropipet was complete so that the sodium reversal potential and the sodium currents were no longer increasing with time. CsTx (18 μl of 4×10^{-6} M) was added to the bathing medium approximately 7 mm from the cell to give a final bath concentration of 1×10^{-7} M. Changes in the time course of the sodium currents were measured during 10 msec test pulses to +10 mV delivered every 30 sec (Fig. 6B). Inactivation of sodium channels was progressively slowed, reaching a new steady state rate of inactivation after 5 min. Fig. 6C shows a family of sodium currents elicited by depolarizations to test potentials of -50 mV to +80 mV 6 min after addition of CsTx. Inactivation of the sodium channels was fully modified by the toxin and the sodium channels did not inactivate completely at the end of the 10 msec test pulse period. Similar slowing of inactivation was observed in all four cells tested at this concentration of toxin. The toxin increased

the peak sodium currents elicited by a test pulse to +10 mV in three of these cells to 120+/-18% (S. D.) of the control level as illustrated in Fig. 6 (compare panels A and C). In contrast to the results with these and all other cells studied, the fourth cell in this group was exceptional and showed a decrease in peak sodium current. The reversal potential of the sodium current was not significantly affected by the toxin (+59.9+/-4.4 mV before toxin, +58.4+/-8.1 mV after toxin) and the toxin-modified currents were completely blocked by 1 x 10^{-6} M tetrodotoxin. These results show that CsTx slows the inactivation of sodium channels and increases peak sodium conductance through the channels.

When CsTx was applied at a lower final concentration of 3 x 10^{-8} M, the time course of sodium channel inactivation had two components, a rapid one corresponding to inactivation of unmodified channels and a slower one corresponding to toxin-modified channels (for examples, see Figs. 9 and 10). Peak sodium currents were also increased at the lower toxin concentration to a mean of 136% of control for two cells studied.

Fig. 7 compares time courses of decay of sodium currents during test pulses to +10 mV for 70 msec in the presence or absence of 1 x 10^{-7} CsTx on semi-logarithmic coordinates. The decay of the sodium currents in the absence of toxin was described by a single exponential with a decay constant of 0.7 msec. In contrast, in the presence of CsTx the sodium current decayed more slowly in a multi-exponential time course. The limiting slope of the first phase of decay was consistent with a time constant of 15.8 msec. Thereafter, the current decayed progressively more slowly, with 12% of the peak sodium current remaining at the end of the 70 msec test pulse period.

Fig. 8 illustrates the relationship between normalized peak sodium conductance and the test pulse potential before and after treatment with 1 x 10^{-7} M CsTx. The potential for half-maximal activation was shifted to more negative membrane potentials by 10.8+/-1.9 mV in four cells. Similar shifts in the conductance-activation curve were observed when the inactivation of sodium currents of N18 neuroblastoma cells was inhibited by treatment with Leiurus scorpion toxin (Gonoi, et al, 1984), Goniopora coral toxin (Gonoi, et al, 1986), or proteolytic enzymes (Gonoi and Hille, in press).

The apparent voltage dependence of inactivation is also altered by CsTx (Fig. 8). In the presence of the toxin, the test pulse potential required for half-maximal inactivation in a 100 msec pulse was shifted to more negative membrane potentials by 13.7+/-6.4 mV in eight cells. Since the time course of inactivation is greatly slowed by CsTx, the inactivation curve determined at 100 msec may not represent the true steady state. Long pre-pulses were not used because slow inactivation becomes important. In all cells tested, the voltage dependence of inactivation measured at 100 msec was less steep in the presence of toxin and inactivation was incomplete, even after a 100 msec prepulse at -20 mV (Fig. 8).

Voltage dependence of CsTx action. The binding and action of several other polypeptide neurotoxins which slow sodium channel inactivation are voltage-dependent including α-scorpion toxins (Catterall, 1977; Gonoi, et al, 1984; Catterall, 1980; Catterall, 1979; Mozhayeva, et al, 1980), sea anemone toxins (Catterall and Beress, 1978; Lawrence and Catterall, 1981; Warashina and Fugita, 1983; Kryshtal, et al, 1982), and Goniopora coral toxin (Gonoi, et al, 1986). In each case, the affinity of these toxins for their receptor sites on the sodium channel is reduced by membrane depolarization. We examined the membrane potential dependence of the action of CsTx by varying the holding potential of the cell as described previously for scorpion and coral toxins (Gonoi, et al, 1984; Gonoi, 1986). Before beginning the recordings, cells were incubated in recording medium containing 3 x 10^{-8} M CsTx for 30 min at 37° to allow equilibrium binding of the toxin. After forming a seal on a cell, the holding potential was maintained

at -80 mV for 10 min and a family of sodium currents was elicited by 10 msec depolarizing test pulses to potentials of -50 mV to +80 mV following 200 msec hyperpolarizing prepulses to -120 mV (Fig. 9A). The sodium currents decayed with a biphasic time course as expected for a mixture of modified and unmodified channels. After changing the holding potential to -40 mV and incubating the cells for 5 min to allow equilibration of the toxin, the extent of modification of the sodium currents was reduced (Fig. 9B). After further depolarization of the holding potential to 0 mV, the time course of the sodium currents returned to essentially that of unmodified channels (Fig. 9C). Hyperpolarization of the membrane potential to -80 mV increased the degree of modification of sodium currents by CsTx to the original level (data not shown). These results demonstrate that the binding and/or action of CsTx is reduced by membrane depolarization in the range of -80 mV to 0 mV.

Similar experiments were carried out over the membrane potential range from -160 mV to -80 mV (Fig. 10). Surprisingly, we found that hyperpolarization of the holding potential beyond -80 mV decreased the fraction of sodium channels that inactivated slowly. To examine this effect more carefully, we carried out experiments starting from a holding potential of -160 mV so that the direction of membrane potential change was the same as in Fig. 9. After incubating cells with 3×10^{-8} M CsTx for 30 min at 37° and hyperpolarizing to -160 mV for 10 min (Fig. 10A), the extent of modification of sodium currents appeared less than in the corresponding experiment at -80 mV (compare Fig. 9A). Depolarization of the holding potential to -100 mV followed by measurement of the sodium current elicited by a single 10 msec test pulse to +10 mV revealed a progressive increase in the slowly inactivating fraction of the sodium current upon depolarization in this membrane potential range (Fig. 10B). The new steady state time course of the sodium current was reached in 5 min. A family of sodium currents elicited at this time showed that, in comparison to the records at a holding potential of -160 mV, the inactivation of the sodium current was slowed at all test potentials , the peak sodium current was increased, and the sodium current was activated at more negative test potentials (Fig. 10C). Thus, the binding and action of CsTx is increased by depolarization of the membrane potential in the range of -160 to -80 mV.

Since unmodified sodium channels inactivate nearly completely by 3 msec after the beginning of a test pulse to +10 mV (see Fig. 7), the fraction of sodium conductance that remains at 3 msec provides an estimate of the fraction of sodium channels with slowed inactivation (Gonoi, et al, 1984). The fraction of sodium conductance remaining at 3 msec is plotted as a function of the holding potential in Fig. 11A. The results at the 9 holding potentials tested define a biphasic dependence of the binding and action of CsTx on membrane potential with maximum effect in the range of -100 to -60 mV. If we assume that the voltage-dependence of the toxin effect is due to voltage-dependence of the affinity for CsTx binding at a single receptor site on the sodium channel protein, as has been shown for α-scorpion toxins and sea anemone toxins (Catterall, 1977; Gonoi, et al, 1984; Catterall, 1980; Catterall, 1979; Mozhayeva, et al, 1980; Catterall and Beress, 1978; Lawrence and Catterall, 1981; Warashina and Fugita, 1983; Kryshtal, et al, 1982), then apparent K_D values for toxin binding at each membrane potential can be calculated from the data of Fig. 11A. As illustrated in Fig. 11B, a plot of the log of the apparent K_D versus membrane potential is also biphasic. At membrane potentials more positive than -60 mV, the apparent K_D increases e-fold for each 19 mV depolarization. The slope is similar to that observed for Leiurus scorpion toxin in the same cells (Gonoi, et al, 1984) as indicated by the straight line in Fig. 11B. At membrane potentials more negative than -100, the apparent K_D is increased 10 fold. A similar increase in the apparent K_D for Leiurus toxin at negative membrane potentials was not observed in our previous experiments (Gonoi, et al, 1984), although we cannot exclude the possibility that it may occur at even more negative membrane potentials than those tested.

Effect of external Na^+ on CsTx action. In previous work, we found that the inhibition of sodium channel inactivation by a polypeptide toxin from the coral Goniopora required Na^+ or another alkali metal cation in the extracellular medium. No effect of the toxin was observed in Na^+-free, choline-substituted medium (Gonoi, et al, 1986). To examine the requirement for extracellular Na^+ for CsTx action, neuroblastoma cells were incubated for 30 min at 37° in sodium-free medium with or without 3×10^{-8} M toxin and outward sodium currents were measured with micropipets containing 135 mM Na^+ as described under Experimental Procedures. Outward sodium currents were markedly prolonged by incubation with CsTx under these conditions (Fig. 12), indicating that extracellular Na^+ is not required for the action of CsTx on sodium channel inactivation.

Site of action of CsTx. Sodium channels have five receptor sites for neurotoxins that have been defined in previous neurotoxin binding studies (reviewed in Catterall, 1980; Catterall, 1984; Catterall, 1985). We have examined the effects of CsTx on specific binding of neurotoxins at three of these sites as an initial step in determination of its site of action.

Neurotoxin receptor site 1 on the sodium channel binds the heterocyclic guanidines tetrodotoxin and saxitoxin which block the sodium conductance of the channel (Catterall, 1980; Ritchie and Rogart, 1977). The polypeptides geographutoxin I and II, μ conotoxins from Conus geographus, specifically block muscle sodium channels by interaction with this same receptor site (Ohizumi, et al, 1986; Moczydlowski, et al, 1986; Yanagawa, et al, 1986). It was of interest therefore to determine whether CsTx also binds at this site. Specific binding of [^{3}H]saxitoxin to this receptor site on sodium channels in rat brain synaptosomes was measured as described under Experimental Procedures. No effect of CsTx on saxitoxin binding was observed at concentrations up to 1×10^{-7} M (Fig. 13), indicating that CsTx does not bind to neurotoxin receptor site 1 on sodium channels.

Neurotoxin receptor site 2 on the sodium channel binds lipid soluble neurotoxins, including batrachotoxin, which cause persistent activation of sodium channels (reviewed in Catterall, 1980; Albuquerque and Daly, 1976). Binding and activation of sodium channels by these toxins is enhanced by polypeptide toxins which inhibit inactivation of sodium channels through an allosteric mechanism (Catterall, 1980; Catterall, 1985; Catterall, 1977). Since CsTx inhibits inactivation of sodium channels, we expected that it would also enhance binding of neurotoxins to neurotoxin receptor site 2. Specific binding of 10 nM [^{3}H]BTX-B was measured as described under Experimental Procedures in a Na^+-free, choline-substituted medium. In the absence of other toxins, CsTx increased specific binding of [^{3}H]BTX-B by 50% with half-maximal effect at a concentration of approximately 1.5×10^{-8} M (Fig. 14). At the membrane potential of synaptosomes (-55 mV), the apparent K_D for inhibition of sodium channel inactivation by CsTx is 1.1×10^{-8} M (Fig. 11B). Thus, the enhancement of specific binding of [^{3}H]BTX-B is observed in the same range of CsTx concentrations that inhibits inactivation of sodium channels. Leiurus α-scorpion toxin enhances specific binding of [^{3}H]BTX-B by as much as 10-fold (Catterall, 1981). In the presence of 3×10^{-7} M Leiurus toxin, CsTx did not cause a detectable further enhancement of [^{3}H]BTX-B binding (Fig. 14). These results suggest a limited allosteric interaction between CsTx and neurotoxins binding at site 2 on the sodium channel.

Neurotoxin receptor site 3 on the sodium channel binds the polypeptides α-scorpion toxin and sea anemone toxin which inhibit sodium channel inactivation and enhance persistent activation of sodium channels by neurotoxins acting at receptor site 2

(reviewed in Catterall, 1980). In order to determine whether CsTx exerts similar effects on the sodium channel by interaction with neurotoxin receptor site 3 as well, we examined the effects of CsTx on specific binding of ^{125}I-labeled Leiurus scorpion toxin as described under Experimental Procedures (Fig. 13). A saturating concentration of CsTx (1×10^{-7} M) reduced specific scorpion toxin binding by only 17%. These results show that CsTx does not occupy neurotoxin receptor site 3 in causing its effects on inactivation of sodium channels, although its binding may reduce the affinity of neurotoxin receptor site 3 for Leiurus scorpion toxin slightly. CsTx must affect sodium channel inactivation by interaction with a site other than neurotoxin receptor sites 1 through 3.

Modification of sodium channel inactivation by toxin action at a new site. Our results establish a fourth class of polypeptide neurotoxins that specifically inhibit inactivation of sodium channels. Early voltage clamp experiments showed that scorpion venoms, and basic polypeptide toxins of approximately 7000 daltons isolated from them, preferentially slow and block sodium channel inactivation (Koppenhofer and Schmidt, 1968; reviewed in Catterall, 1980). These toxins bind in a voltage-dependent manner to a single receptor site (receptor site 3) on the sodium channel (Catterall, 1977; Catterall, 1980; Catterall, 1979) and enhance, through an allosteric mechanism, the activation of sodium channels by lipid soluble neurotoxins like batrachotoxin which act at neurotoxin receptor site 2. Basic polypeptides of 3000 to 5000 daltons from sea anemone nematocysts also preferentially slow or block sodium channel inactivation (reviewed in Catterall, 1980) and bind to neurotoxin receptor site 3 in a voltage-dependent manner (Catterall and Beress, 1978; Lawrence and Catterall, 1981; Warashina and Fugita, 1983; Kryshtal, et al, 1982). In contrast to these two classes of toxins which exert their effects on sodium channel inactivation by binding at receptor site 3, recent results show that a polypeptide of 10,000 daltons from the coral Goniopora inhibits sodium channel inactivation by voltage-dependent interaction with a different receptor site (Gonoi, et al, 1986), and the results presented in this report demonstrate that a polypeptide of approximately 25,000 daltons isolated from the venom of the marine snail Conus striatus has a similar action. It is of interest to compare the physiological actions of these four structurally distinct classes of toxins.

The common denominator of the action of all four classes of toxins is their ability to slow sodium channel inactivation markedly without altering the time course of channel activation. This action is usually accompanied by three other effects: a reduction in the steepness of the voltage dependence of steady state inactivation for α-scorpion toxins, sea anemone toxins, and CsTx, but not for Goniopora toxin (Gonoi, et al, 1984; Gonoi, et al, 1986; Mozhayeva, et al, 1980; Catterall and Beress, 1978; Warashina and Fugita, 1983; Kryshtal, et al, 1982; Koppenhofer and Schmidt, 1968; Bergman, et al, 1976); incomplete inactivation after long depolarizing pulses to positive membrane potentials for all four classes of toxin (Gonoi, et al, 1984; Gonoi, et al, 1986; Mozhayeva, et al, 1980; Koppenhofer and Schmidt, 1968; Bergman, et al, 1976); and a shift in the voltage dependence of steady state inactivation to more negative membrane potentials for CsTx (this work) or more positive membrane potentials for Goniopora toxin (Gonoi, et al, 1986).

These toxins alter the voltage dependence of activation and increase the peak sodium current in N18 neuroblastoma cells (Gonoi, et al, 1984; Gonoi, in press; Catterall, 1980). These effects are also evident when inactivation is blocked by treatment with proteolytic enzymes or with chemical reagents (Gonoi and Hille, in press). Thus, these effects should be considered secondary consequences of the primary effect of the toxins to slow inactivation. Inactivation of sodium channels in N18 cells is very rapid and is not strongly voltage-dependent (Gonoi and Hille, in press). Inactivation therefore

abbreviates the rise of the sodium current before maximum activation is achieved. The peak sodium current increases and the voltage dependence of activation shifts to more negative membrane potentials when inactivation is slowed or blocked because the increase in sodium current after depolarization attains the full level allowed by the voltage dependence of sodium channel activation without attenuation by inactivation. Kinetic models which account for this behavior have been discussed previously by Gonoi and Hille (in press).

Voltage-dependent binding and/or action is also a common feature of the mechanism of these four classes of toxins. However, the voltage dependence differs quantitatively among the toxins that have been studied. The K_D for binding of Leiurus toxin increases e-fold for each 15 to 21 mV depolarization and there is a linear relationship between the log of K_D and membrane potential over a wide range (Catterall, 1977; Gonoi, et al, 1984; Catterall, 1979; Mozhayeva, et al, 1980). The voltage dependence of sea anemone toxin action is similar with an e-fold increase in apparent K_D for each 15 mV depolarization over the range that has been examined (Kryshtal, 1982). Goniopora coral toxin has a shallower voltage dependence with an e-fold increase in apparent K_D for each 48 mV depolarization (Gonoi, et al, 1986). However, the change in apparent K_D with hyperpolarization appears to level off at potentials more negative than -100 mV. The voltage dependence of CsTx action differs even more markedly from a log-linear relationship between apparent K_D and membrane potential (Fig. 6). Between -60 mV and 0 mV, K_D increases e-fold per 19 mV depolarization as for Leiurus scorpion toxin. However, at more negative membrane potentials, K_D decreases to a minimum value and then begins to increase again. What mechanisms might account for the widely differing voltage dependence of the binding and action of these toxins which all inhibit sodium channel inactivation? The voltage dependence of Leiurus toxin action results from preferential binding to activated states of sodium channels (Catterall, 1977; Catterall, 1979). Current models of sodium channel gating indicate that the channel protein must undergo several voltage-dependent transitions connecting discrete nonconducting states before activation of the channel can occur (Armstrong, 1981; Catterall, 1986). Inactivation of the channel may occur from one or more of these nonconducting states as well as from the activated state of the channel. The different voltage-dependence of binding and action of the toxins which inhibit inactivation may result from preferential binding of these different toxins to different states along the pathway toward the activated and inactivated states of the channel. Since the fraction of sodium channels that is in each of these states is expected to have different voltage dependence for each state, toxins which have preferential affinity for different channel states would be expected to have different voltage dependence of binding.

α-scorpion toxins and sea anemone toxins share a common receptor site, neurotoxin receptor site 3, on the sodium channel protein (Catterall, 1980; Catterall, 1978). In contrast, Goniopora toxin and CsTx act at one or more different receptor sites. The sites of Goniopora toxin action and CsTx action may be separate from one another since extracellular Na^+ is required for Goniopora toxin action but not for CsTx action and the voltage dependence of toxin action at the two sites is distinctly different. Evidently, there are multiple sites on the extracellular surface of the sodium channel at which inactivation can be altered, and each of these receptor sites can undergo voltage dependent conformational changes during the transition from resting to activated sodium channels. Identification of these receptor sites at the molecular level may provide insight into the structural changes which take place during channel activation and inactivation.

B. Site-directed Antibodies as Probes of Sodium Channel Structure and Function

Neurotoxins act at multiple discrete receptor sites on the sodium channel protein. Most of these are located on the α subunit whose primary structure is known. We have sought to design site-directed antibodies against known segments of the α subunits of the α subunit with three objectives in mind: (1) to determine the tissue distribution of sodium channel subtypes having an amino acid sequence identical or highly homologous to those whose primary structures are known; (2) to identify the sites of neurotoxin action on sodium channels in key target tissues for neurotoxin action; and (3) to design antibody reagents to interdict neurotoxin action in their most sensitive target tissues. In the past year, we have made substantial progress on the first two of these objectives.

1. Tissue-specific Expression of the R_I and R_{II} Sodium Channel Subtypes

Sodium channels isolated in functional form from rat brain, rat and rabbit skeletal muscle, and electric eel electroplax all contain a large glycoprotein subunit of 260 kDa as their principal component (reviewed in Agnew, 1984; Barchi, et al, 1984; Catterall, 1984; Catterall, 1986). In brain and skeletal muscle, this α subunit is associated with one or two smaller β subunits (Catterall, 1984; Catterall, 1986). cDNA clones encoding the primary structure of the α subunits from electroplax (Noda, et al, 1984) and rat brain (Auld, et al, 1985; Mandell, et al, 1986; Noda, et al, 1986; Goldin, et al, 1986) have been isolated, and the complete primary structures of α subunits from electroplax and rat brain have been determined (Noda, et al, 1984; Noda, et al, 1986). High molecular weight mRNA from rat brain (Sumikawa, 1986), α subunit mRNA isolated by hybrid selection (Goldin, et al, 1986), and α subunit mRNA synthesized from cloned cDNA (Noda, et al, 1986) all direct the synthesis of functional sodium channels in *Xenopus* oocytes. Two recent lines of investigation indicate that there are multiple subtypes of sodium channels expressed in mammalian neurons. Polyclonal antibodies directed against the α subunit of the rat brain sodium channel do not recognize sodium channels in peripheral neurons (Wollner and Catterall, 1985). Moreover, cDNA clones encoding three different α subunit mRNA's have been detected in rat brain, and two of these have been fully sequenced (Noda, et al, 1986). These two mRNA's encode R_I and R_{II} α subunit subtypes having 87% identity in their predicted amino acid sequence. In these studies, we have analyzed the tissue-specific expression of the R_I and R_{II} sodium channel subtypes using sequence-directed antibodies that distinguish these two forms.

Synthetic peptides. SP1 (CAYEEQNQATLEEAENKEA), corresponding to residues 425-442 of R_I (Noda, et al, 1986) or residues 427-444 of R_{II} (Noda, et al, 1986) plus an N-terminal cys extension, SP11$_I$ (KTASEHSKETSAAGRLSD), corresponding to residues 465-481 of R_I (Noda, et al, 1986) plus an N-terminal lys extension, and SP11$_{II}$ (KASAESRDFSGAGGIGVFSE), corresponding to residues 465-484 (Noda, et al, 1986) plus an N-terminal lys extension were synthesized by the solid phase method (Merrifield, 1963) and purified by reversed phase HPLC on a Vydac 218TP10 column. The identity of the purified peptides was verified by amino acid analysis and by determination of amino acid sequence. SP1 was radiolabeled with ^{125}I by the chloramine T method (Hunter and Greenwood, 1962); SP11$_I$ and SP11$_{II}$ were radiolabeled by reaction with the Bolton-Hunter reagent (Bolton and Hunter, 1973).

Preparation of antibodies. The purified peptides were coupled through amino groups to bovine serum albumin with glutaraldehyde (Orth, 1979), dialyzed against phosphate buffered saline, emulsified in an equal volume of Freund's complete (initial injection) or incomplete adjuvant, and injected in multiple subcutaneous sites on New Zealand white rabbits at three week intervals. Antisera were collected after the second

injection and tested by radioimmune assay (Costa and Catterall, 1984). Antibodies were purified by antigen affinity chromatography (Wollner and Catterall, 1984; Olmsted, 1981).

Preparation of tissue fractions. A crude synaptosomal membrane fraction (P_3) was prepared from whole rat brain as described previously (Catterall, et al, 1979). Electric eel brain and regions of rat brain were homogenized in 3.3 ml per g tissue of sucrose buffer consisting of 5 mM EDTA, 5 mM EGTA, 300 mM sucrose, pH 7.4, 50 μg/ml phenyl methanesulfonyl fluoride, 1 μM pepstatin A, and 1 mM iodoacetamide. Debris was removed by centrifugation at 800 xg for 10 min and the membranes were collected by centrifugation at 100,000 xg for 60 min. Brains from monkey, chicken, gecko, and frog were homogenized in 320 mM sucrose, 5 mM potassium phosphate, pH 7.4, 1.5 μM phenylmethanesulfonyl fluoride, 1 μM pepstatin A, and 1 mM iodoacetamide. Freshly dissected retinae and optic nerves were homogenized in 130 mM choline chloride, 5.4 mM KCl, 0.8 mM $MgCl_2$, 5.5 mM glucose, 50 mM HEPES-Tris, pH 7.4, 50 μg/ml phenylmethanesulfonyl fluoride, 1 μM pepstatin A, and 1 mM iodoacetamide. Frozen superior cervical ganglia, adrenal medullae, and sciatic nerves (Rockland Scientific) were rapidly thawed and homogenized in sucrose buffer. Rat skeletal muscle was dissected from the hind legs and a light surface membrane fraction was prepared by a modification of the method of Barchi et al (1979). Sodium channel concentration was determined by measurement of specific binding of saxitoxin in membrane fractions at 0°C using a rapid filtration assay on GF/F filters at 20 nM saxitoxin (Catterall, et al, 1979).

Solubilization, immunoprecipitation, and phosphorylation of sodium channels. Membrane fractions were diluted to 1 nM sodium channels (100 fmol per sample) as assessed by saxitoxin binding activity in solubilization buffer consisting of 100 mM choline chloride, 10 mM EDTA, 10 mM EGTA, 50 mM potassium phosphate, pH 7.4, and 3% to 5% Triton X-100 plus the protease inhibitors phenylmethylsulfonylfluoride (50 μg/ml), iodoacetamide (1 mM), and pepstatin A (1 mM). After mixing for 30 min at 4°C, the residual membranes were sedimented at 8000 x g for 15 min. The supernatants were incubated for 16 hr with affinity-purified antibodies at 4°C. The antigen-antibody complexes were isolated by adsorbtion to protein A-Sepharose (10 mg) and the pellets were washed twice with phosphorylation buffer (Schmidt, et al, 1985). The immunoprecipitated sodium channels were radiolabeled by phosphorylation with 500 ng cAMP-dependent protein kinase and 5 μCi [γ-^{32}P]ATP for 1 min at 36°C (Schmidt, et al, 1985).

NaDodSO4 gel electrophoresis. Pellets from immunoprecipitation and phosphorylation were suspended in sample buffer consisting of 3% NaDodSO4, 30 mM Tris (adjusted to pH 8.6 with HCl), 2 mM EDTA, 5% sucrose, and 5% β-mercaptoethanol and boiled for 5 min. The pH was adjusted to 7.4 and the proteins were resolved by electrophoresis through a stacking gel of 3% acrylamide and a running gel with a 3% to 10% acrylamide gradient as previously described (Schmidt, et al, 1985; Maizel, 1971). Radiolabeled bands were visualized by autoradiography. The intensity of autoradiographic bands was determined with a Soft Laser Scanning densitometer (Zeineh SL-504-XL). Exposure times were selected to give a linear response of the film to the incorporated radioactivity.

Specific recognition of R_I and R_{II}. Affinity-purified antibodies were prepared against a peptide (SP1) corresponding to a conserved sequence in the R_I and R_{II} sodium channel subtypes and against two peptides ($SP11_I$ and $SP11_{II}$) corresponding a nearby divergent sequence having only three widely spaced amino acids out of 18 that are common between these subtypes. Immunoprecipitation of purified, ^{32}P-labeled sodium

channels by increasing concentrations of the antibodies against the SP1 and SP11 peptides is illustrated in Fig. 15A. At saturating concentrations, anti-SP11I antibodies precipitated 26% and anti-SP11II antibodies precipitated 70% of the ^{32}P-labeled sodium channels that were precipitated by anti-SP1 (Fig. 15A). Immunoprecipitation by saturating concentrations of anti-SP11I and anti-SP11II was additive indicating that these antibodies immunoprecipitate different populations of purified sodium channels (Fig. 15B).

The crossreactivity of the anti-SP11I and anti-SP11II antibodies was examined in the experiment illustrated in Fig. 16. Immunoprecipitation of ^{32}P-labeled sodium channels by anti-SP11I is reduced to 50% of maximum by 2.5 nM SP11I or 11.5 nM unlabeled sodium channels, which corresponds to approximately 2.9 nM RI. Saturating concentrations of unlabeled sodium channels or SP11I completely block immunoprecipitation by anti-SP11I, but similar concentrations of SP11II have no effect. Similarly, immunoprecipitation of ^{32}P-labeled sodium channels by anti-SP11II is reduced to 50% of maximum by 0.5 nM SP11II or 0.8 nM sodium channels which corresponds to approximately 0.6 nM RII. Saturating concentrations of unlabeled sodium channels or SP11II completely block immunoprecipitation by anti-SP11II, but SP11I has no effect. These results show that these anti-peptide antibodies bind native sodium channels almost as well as the peptides used as antigens and that they are specific for distinct α subunit subtypes present in the purified sodium channel preparation from rat brain. It is likely that they recognize specifically the RI and RII sodium channel subtypes whose primary structures contain the corresponding amino acid sequences.

Measurement of RI and RII by immunoprecipitation and phosphorylation. The α subunits of rat brain sodium channels are unusually good substrates for phosphorylation by cAMP-dependent protein kinase (Costa and Catterall, 1984) and both the RI and RII subtypes are readily phosphorylated *in vitro* (Fig. 15). The phosphorylation sites of these two channel subtypes are located on the same set of tryptic phosphopeptides, indicating that RI and RII are phosphorylated on the same sites (Rossie and Catterall, manuscript in preparation). Immunoprecipitation of sodium channels with specific antibodies, radiolabeling of the precipitated α subunits by phosphorylation with cAMP-dependent protein kinase, and analysis by SDS-PAGE provides a sensitive method for detection of sodium channels in neuronal tissues, allowing detection of 2 fmol of sodium channels in unpurified membrane extracts (Schmidt, et al, 1985). In these experiments, we have adapted this method to analyze tissue-specific expression of the RI and RII sodium channel subtypes using sequence-specific antibodies.

Sodium channels were solubilized from a lysed crude synaptosomal membrane fraction (lysed P3) from rat brain, immunoprecipitated with anti-SP1, anti-SP11I, or anti-SP11II antibodies, phosphorylated, and analyzed by SDS-PAGE. One major phosphorylated protein band of 260 kDa is observed with each antibody (Fig. 17, lanes 1-3), but not with preimmune antiserum or with affinity-purified antibodies that have been previously blocked by incubation with the corresponding peptide antigen (data not shown). Therefore, this band represents the α subunits of the sodium channel. Anti-SP1 immunoprecipitates more labeled α subunits than either of the antibodies directed against variable sequences of the protein (Fig. 17A, lane 1). In analyzing our results, we have set the amount of radiolabeled α subunits immunoprecipitated by anti-SP1 antibodies equal to 100% (Fig. 15A) and have compared the amounts precipitated by anti-SP11I and anti-SP11II to that value. By this criterion, RI and RII comprise an average of 15.1% and 60.4%, respectively, of sodium channels in membrane preparations from whole rat brain.

Several control experiments were carried out to examine whether our methods provide an accurate measurement of the ratio of expression of these two channel

subtypes. Experiments with increased concentrations of antibodies confirmed that the amounts used were saturating. Measurements of the dissociation rates of the antibody-^{32}P-labeled sodium channel complex during subsequent centrifugation, phosphorylation, and washing showed that complexes with anti-SP1 and anti-SP11$_I$ antibodies are recovered quantitatively, while approximately 30 % of complexes with anti-SP11$_{II}$ antibodies are lost. We have applied a correction factor to account for this in quantitatively analyzing our results in Table 1 and Fig. 19. With this correction, our results indicate that the sodium channels in crude synaptosomal membrane preparations from whole rat brain are 15% R$_I$ and 78% R$_{II}$. Comparison of these values with those for purified preparations (Fig. 15A) suggests that the R$_I$ subtype is recovered in higher yield during purification.

Variations in the extent of endogenous phosphorylation of sodium channel subtypes or in dephosphorylation of these subtypes during tissue fractionation might influence the extent of radiolabeling of sodium channels in tissue extracts by phosphorylation. Purified R$_I$ and R$_{II}$ sodium channels are rapidly dephosphorylated by phosphatases in rat brain cytosolic fractions (Rossie and Catterall, unpublished experiments). Prior dephosphorylation of the sodium channels in extracts of rat brain and spinal cord, which have widely differing ratios of R$_I$ to R$_{II}$ (see below), by incubation with a rat brain cytosol fraction before immunoprecipitation and radiolabeling had no effect on the ratios of R$_I$ and R$_{II}$ observed. Similarly, prior dephosphorylation of sodium channels from tissues in which these subtypes were not detected (see below) did not reveal either subtype. The extents of dephosphorylation of the cAMP-dependent phosphorylation sites on R$_I$ and R$_{II}$ during tissue preparation, solubilization, and incubation with antibodies were measured by addition of purified, ^{32}P-labeled sodium channels and found to be comparable. Thus, differential endogenous phosphorylation and differential dephosphorylation of sodium channel subtypes during tissue fractionation do not influence the results described below.

R$_I$ and R$_{II}$ are expressed differentially in the central nervous system. Similar analyses of the amounts of R$_I$ and R$_{II}$ were carried out with tissue samples containing 100 fmol of saxitoxin binding sites from specific regions of the central nervous system. As illustrated in Fig. 17, hippocampus, cerebral cortex, and cerebellum expressed substantially less R$_I$ than R$_{II}$ with R$_I$/R$_{II}$ ratios ranging from 0.07 in the hippocampus to 0.17 in cerebral cortex (Table 1). In these brain regions, R$_I$ and R$_{II}$ accounted for greater than 90% of the sodium channels recognized by anti-SP1, the antibody we have used to define 100% in these studies. If other sodium channel subtypes are present in these brain regions, they must comprise only a small portion of the total, lack phosphorylation sites, or fail to be recognized by these three sequence-directed antibodies and our other polyclonal antibodies. In the midbrain, R$_{II}$ is also expressed at a higher level than R$_I$ (Fig. 17, Table 1). However, sodium channels that are recognized by anti-SP1 but not by anti-SP11$_I$ or anti-SP11$_{II}$ are also detected (Table 1). Nevertheless, expression of the R$_{II}$ subtype is clearly predominant in these higher brain regions among the sodium channel subtypes that are detected by the methods used here.

In contrast, R$_I$ was expressed at comparable or higher levels than R$_{II}$ in medulla oblongata and spinal cord with R$_I$/R$_{II}$ ratios of 0.98 and 2.2, respectively (Fig. 17 and Table 1). In addition, in these more caudal regions of the central nervous system, unidentified sodium channel subtypes that are recognized by anti-SP1 antibodies but not by anti-SP11$_I$ or anti-SP11$_{II}$ antibodies comprised a substantial fraction of the sodium channels detected. Therefore, expression of both the R$_I$ subtype and of unidentified subtypes of sodium channels in medulla oblongata and spinal cord is increased relative to the R$_{II}$ subtype. Since the medulla oblongata contains a substantial complement of

ascending projections from neurons in the spinal cord, much of the R_I sodium channel subtype observed in the medulla could be synthesized by spinal neurons.

The optic nerve and retina are also considered projections of the central nervous system. As in the brain, R_{II} was expressed preferentially compared to R_I with expression ratios of 0.09 and 0.36, respectively (Fig. 17 and Table 1). However, in contrast to other regions of the central nervous system, unidentified sodium channel subtype(s) were the predominant forms expressed in optic nerve and retina accounting for 64% and 76% of the sodium channels detected, respectively.

R_I and R_{II} are expressed primarily in the central nervous system. In previous studies, we have shown by radioimmune assay that sodium channels in the peripheral nervous system and skeletal muscle are poorly recognized by polyclonal antibodies against rat brain sodium channels (Wollner and Catterall, 1985). To extend these previous studies, we first examined whether the sodium channels in several peripheral excitable tissues were recognized by the anti-SP1 antibodies which are directed against a conserved epitope common to R_I, R_{II}, and additional unidentified sodium channels subtype(s) expressed in the central nervous system. These sodium channel subtypes were not detected by immunoprecipitation and phosphorylation with anti-SP1 antibodies in samples containing 100 fmol of saxitoxin binding sites from skeletal muscle (Fig. 18) or heart (data not shown), suggesting that they are expressed primarily in the nervous system. Similarly, these channel subtypes also were not detected in sympathetic ganglia or adrenal medulla (Fig. 18), suggesting that R_I and R_{II} are not expressed by neurons of the autonomic nervous system or by endocrine cells. Moreover, neither R_I, R_{II}, nor the additional unidentified sodium channel subtypes recognized by anti-SP1 antibodies in the central nervous system were detected in sciatic nerve, which contains the peripheral projections of spinal motor neurons, or in cauda equina, the most caudal segment of the spinal cord which contains fiber tracts within the lower vertebrae (Fig. 18), although they are expressed in the central myelinated fibers of the optic nerve (Fig. 17) and corpus callosum (data not shown). Thus, previous results (Wollner and Catterall, 1985) and the work presented here suggest that these channel subtypes are expressed primarily, if not exclusively, by neurons in the central nervous system and are excluded from the peripheral projections of central neurons.

Since expression of the R_I and R_{II} sodium channel subtypes is restricted to the central nervous system, it was of interest to examine whether the antigenic epitopes that we have used to define these subtypes are conserved in the central nervous systems of a range of species. Sodium channels that are recognized by anti-SP1 antibodies were detected in mammalian (rat and monkey), avian (chicken), reptilian (gecko), and amphibian (frog) brains, but not in a bony fish (electric eel) brain (Fig. 17B). However, sodium channels that are recognized by anti-SP11$_I$ or anti-SP11$_{II}$ were observed only in monkey and rat brain. Although only a few species have been examined, it appears that these epitopes may be conserved among mammals but are not conserved in most nonmammalian vertebrates.

Expression of R_I and R_{II} is differentially regulated during development. Analysis of the relative expression of R_I and R_{II} in brain and spinal cord during development reveals additional levels of regulation (Fig. 19). At birth, the number of sodium channels in rat or mouse brain per unit wet weight, as measured by high affinity binding of saxitoxin, is less than 10% of the adult level (Unsworth and Hafemann, 1975; Baumgold, et al, 1983; Lombet, et al, 1984). The density of sodium channels per unit wet weight in brains with cerebella removed increases steadily during the first 28 days after birth reaching 1.8 times the adult level and declines thereafter returning to the adult level by 90 days. The time course of development of total sodium channels is paralleled by the time

course of appearance of sodium channels of the R_{II} subtype (Fig. 19). R_{II} is present at approximately 7% of the adult level at birth, increases to 1.8 times the adult level by days 21 through 28 and declines toward the adult value by day 90. In contrast, R_I is not clearly detectable until 14 days after birth and increases to the adult level by 28 days (Fig. 19A). The ratio of R_I to R_{II} increases steadily over the entire time course of development that we have examined, increasing from 0 on day 7 to 0.19 on day 90 (Fig. 19B).

We also examined the expression of R_I and R_{II} in newborn and adult spinal cord (Fig. 19B). As in brain, R_{II} was preferentially expressed in the newborn spinal cord and expression of R_I increased progressively during development in the adult. In contrast to brain, expression of R_{II} was reduced in adult and R_I was the predominant subtype expressed.

Tissue-specific expression of sodium channel subtypes. Three or more different sodium channel subtypes are expressed in the rat central nervous system: R_I, R_{II}, and at least one unidentified subtype that is recognized by anti-SP1 antibodies but not by anti-$SP11_I$ or anti-$SP11_{II}$ antibodies. The unidentified subtype we have detected in the central nervous system in our immunoprecipitation experiments may be encoded by the third sodium channel mRNA which Noda et al (1986) detected in rat brain cDNA libraries but did not sequence fully. R_I is preferentially expressed in the spinal cord, R_{II} is preferentially expressed in the brain, and the unidentified subtype(s) recognized by anti-SP1 antibodies are preferentially expressed in retina and optic nerve and to a lesser extent in the spinal cord. In addition to these three or more sodium channel subtypes in the central nervous system, our results provide clear evidence that the sodium channels which are expressed in the peripheral nervous system represent one or more distinct subtypes. Polyclonal antibodies against rat brain sodium channels and anti-peptide antibodies directed against the SP1, $SP11_I$, and $SP11_{II}$ segments of the α subunit all recognize sodium channels in the central nervous system but not in the peripheral nervous system (Wollner and Catterall, 1985, and this paper). Sodium channel subtypes other than R_I and R_{II} must also be expressed in skeletal and cardiac muscle because our experiments with specific antibodies do not detect R_I or R_{II} in muscle tissues (Wollner and Catterall, 1985 and Fig. 18). Correlation of differences in pharmacological and physiological properties with differences in the primary structure of these six or more sodium channel subtypes is an important area for future work.

2. Identification of the α-Scorpion Toxin Receptor Site

We have previously developed methods to covalently label the α-scorpion toxin receptor site on purified and reconstituted sodium channels (Feller, et al, 1985). These methods used an azidonitrobenzoyl derivative of the α-scorpion toxin from *Leiurus quinquestriatus*. Unfortunately, the yield of specifically photolabeled α subunits is quite low when purified and reconstituted sodium channels are labeled with this derivative. Moreover, the allosteric regulation of α-scorpion toxin binding by batrachotoxin, veratridine, and other neurotoxins binding at neurotoxin receptor site 2 on the sodium channel is not observed with the azidonitrobenzoyl derivative. We have now addressed both of these potential problems by synthesis of a new photoreactive derivative with methyl-4-azidobenzimidate. This reagent retains the positive charge of the amino group in the resulting imidate product. This new derivative labels the α subunit of the sodium channel specifically and the extent of labeling is increased in the presence of batrachotoxin and batrachotoxin plus tetrodotoxin as illustrated in Figure 20. The level of incorporation of the methylazido benzimidate derivative is comparable to or greater than the previous azidonitrobenzoyl derivative. The improved specificity of labeling of

purified sodium channels together with better retention of the binding characteristics of native α-scorpion toxins will make this new toxin derivative valuable in our experiments designed to locate their receptor site.

In order to locate the site of covalent attachment of α-scorpion toxins, we have identified several proteases which are effective in cleavage of sodium channel α subunits but do not cleave the α-scorpion toxin label. From these results, we have selected *Staphylococcus aureus* protease V8 for further studies. Cleavage of the sodium channel with V8 protease yields a labeled protein fragment of 70 kDa (Fig. 20) that is detected as a single broad band in SDS-PAGE. Treatment with neuraminidase reduces this fragment to 50 kDa indicating that it is heavily glycosylated (Fig. 22). The substantial level of carbohydrate on this fragment demonstrates that it contains extracellular segments of the channel as expected for the region containing the scorpion toxin binding site.

Our strategy to localize this segment of the α subunit that is covalently labeled by α-scorpion toxins takes advantage of the extensive battery of site-directed antibodies that we have prepared against different segments of the sodium channel. Table 2 summarizes the different site-directed antibodies we have prepared, their sites of binding in the sodium channel sequence, and their immunoprecipitation of the labeled 50 kDa fragment of the α subunit. The various antibodies are arranged in sequence from N-terminal to C-terminal. As illustrated in Table 2, antibodies to peptides SP1, SP8, and SP10 recognize and immunoprecipitate the labeled detectable levels of this fragment is between amino acid residues 205 and 250, while its C-terminus is between amino acid residues 427 and 486. This region contains two small and one major extracellular loop within the first homologous domain of the sodium channel. Six potential sites of N-glycosylation are located in this region.

These results define a major locus of interaction of α-scorpion toxins with the sodium channel. We are now characterizing additional cleavage procedures to produce progressively smaller fragments of the α subunit. These fragments will then be identified by immunoprecipitation with our existing set site-directed antibodies. When we have further localized the site of covalent attachment of the α-scorpion toxin, new site-directed antibodies will be prepared to specifically target those sites. This approach will allow us to determine the site of covalent attachment of scorpion within approximately 20 amino acid residues.

Table I. Differential expression of R_I and R_{II} in the central nervous system

REGION	R_I (%)	R_{II} (%)	UNIDENTIFIED (%)	R_I/R_{II}
Whole Brain				
Purified Na Channels	18	81	<10	0.22
P3 Membranes	15	78	<10	0.19
Cerebral cortex	14	79	<10	0.17
Hippocampus	6	97	<10	0.07
Cerebellum	8	84	<10	0.09
Midbrain	9	56	35	0.16
Medulla oblongata	38	39	23	0.98
Spinal cord	39	18	43	2.18
Optic nerve	3	33	64	0.09
Retina	6	18	76	0.36

Autoradiograms iike those in Figure 17 were scanned under conditions where intensity was proportional to input protein and the density of the α subunit bands was quantitated. The intensity of the α band immunoprecipitated by anti-SP1 antibodies was set at 100% and the amounts of R_I and R_{II} were estimated by comparison with that value using the correction factor described in the text.

TABLE II

Immunoprecipitation of the Scorpion Toxin-Labeled Fragment by Site-Directed Antibodies

Residue	Peptide No.	Immunoprecipitation
30-47	SP16	-
205-211	SP4	-
232-250	SP10	+
317-334	SP8	+
427-445	SP10	+
468-486	SP11	-
1144-1164	SP20	-
1491-1507	SP19	-
1729-1748	SP13	-
1987-2005	SP12	-

Arg-Asp-Cys-Cys-Thr-Hyp-Hyp-Arg-Lys-Cys-Lys-

Asp-Arg-Arg-Cys-Lys-Hyp-Met-Lys-Cys-Cys-Ala-NH_2

Figure 1. Primary structure of GTX II.

Figure 2. Sodium currents of a rat myoball under voltage-clamp conditions before and after applying GTX II. **A.** A family of sodium currents from myoball in a 13 day old culture was recorded 10.5 min after making a seal between the myoball and a micropipet from a holding potential of -100 mV. **B.** 167 µl of 10 µM GTX II in recording medium was applied from the outside of the myoball to give a final concentration of the toxin in the bath of 2.5×10^{-6} M. Reduction of the sodium current after applying the toxin was monitored every 10 sec by depolarizing the myoball to a test pulse potential of -20 mV for 7 msec following a prepulse to -160 mV for 100 msec. The photograph presented was taken 3 min after applying GTX II and shows superimposed sodium currents. The peak sodium current decreased with each measurement after applying toxin until a new steady state was attained in 2 min. **C.** A family of sodium currents 5 min after the application of GTX II from the same cell as in A and B. Stimulus conditions were same as in A. The calibration is common from A to C.

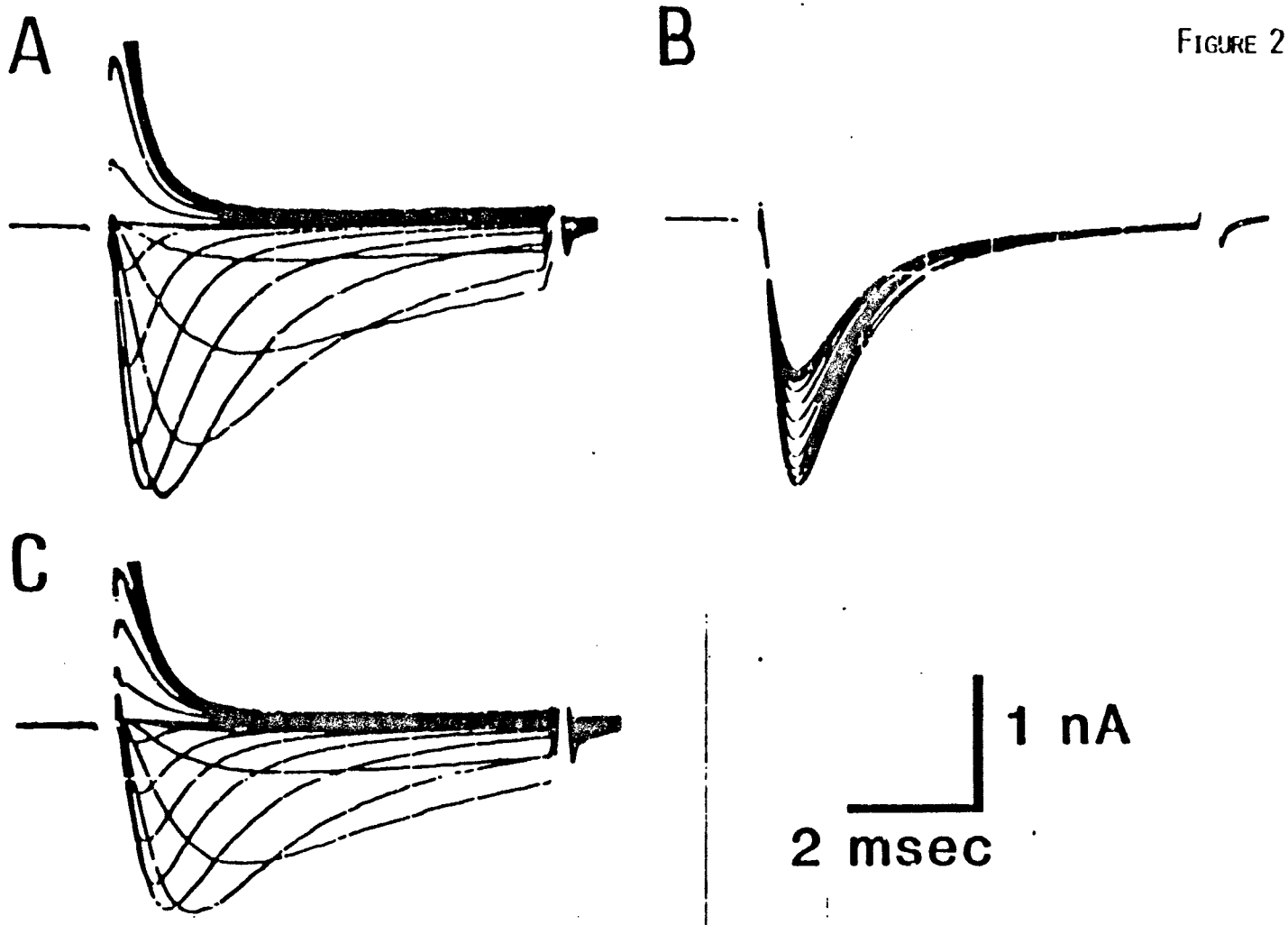

FIGURE 2

Figure 3. Inhibition of sodium conductance in individual myoballs by GTX II. Sodium currents were recorded from two 12 day old myoballs. For each point, GTX II was added from a stock solution of 60 mM in recording medium to achieve the final concentrations indicated. The smooth curves correspond to a least squares fit of the data assuming a one-to-one binding of GTX II to a fraction (F) of sodium channels: △, F = 0.35, K_D = 21 nM,; ○, F = 0.61, K_D = 27 μM.

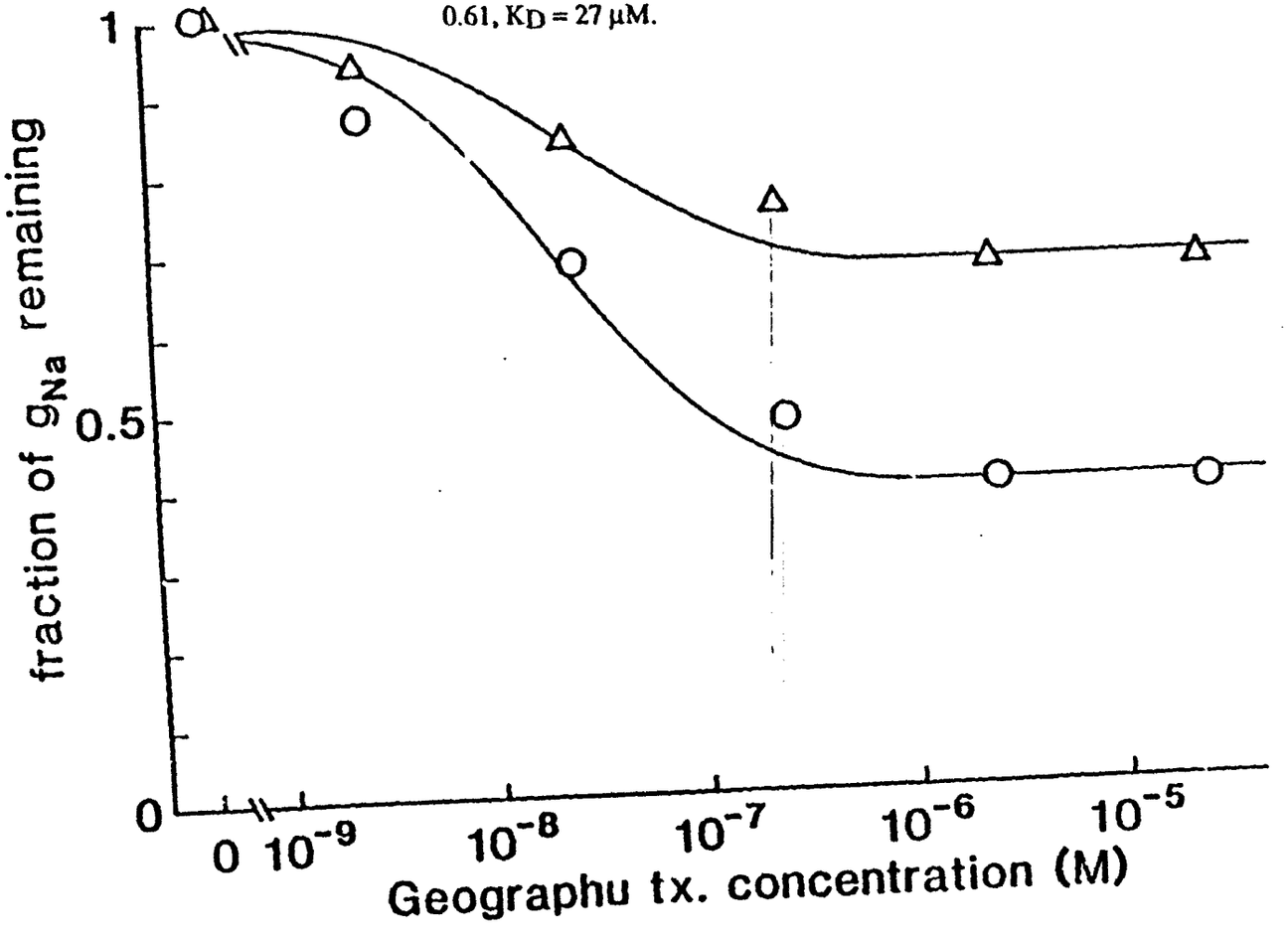

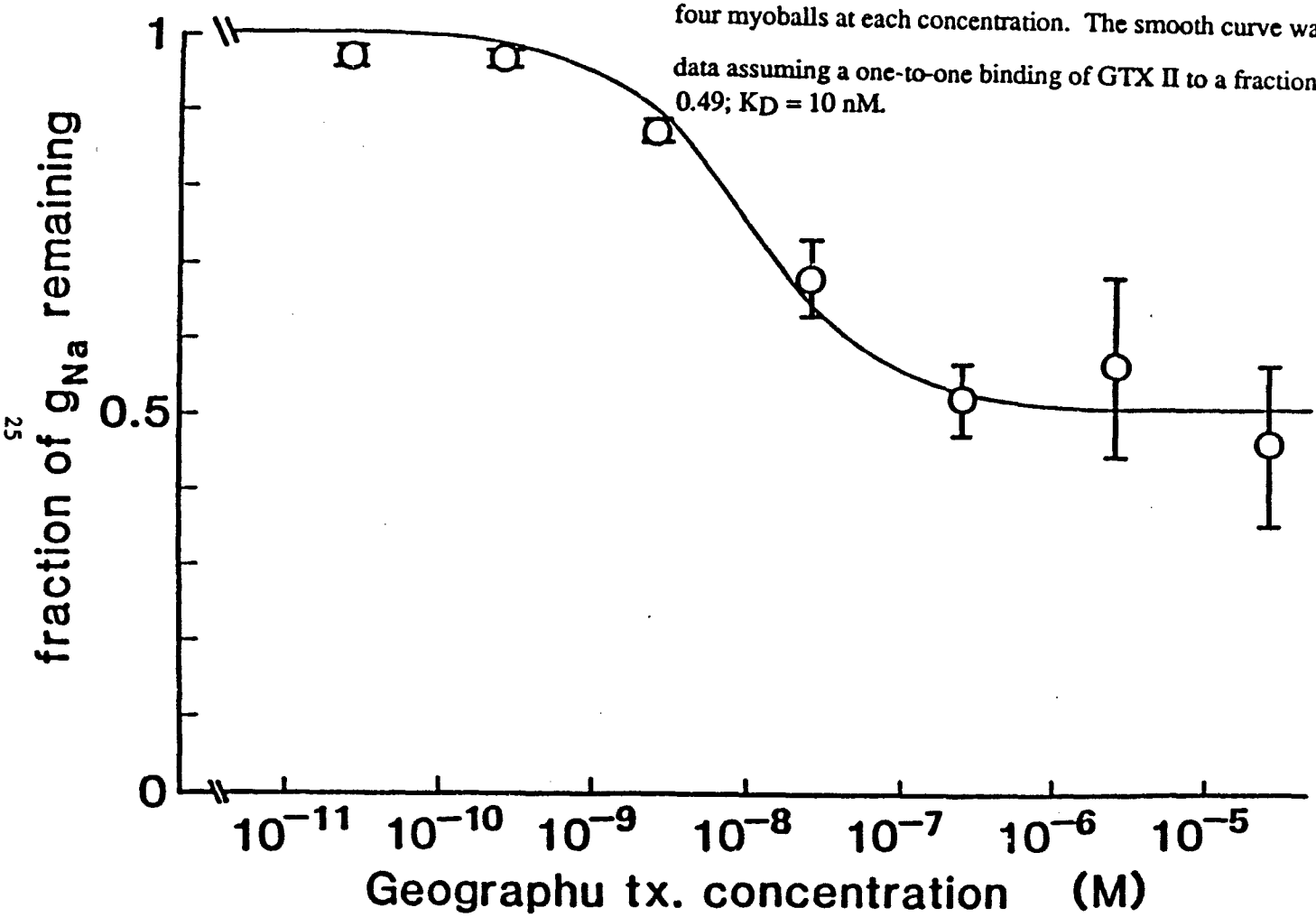

Figure 4. Concentration dependence of inhibition of sodium conductance by II. Sodium currents were recorded from 28 myoballs. For each myoball, currents were r in recording medium and then in recording medium containing the indicated concentratio GTX II. The fraction of sodium conductance remaining in the presence of GTX II was calculated at each toxin concentration and the mean (±S.D) was calculated from the resu four myoballs at each concentration. The smooth curve was obtained by a least squares f data assuming a one-to-one binding of GTX II to a fraction (F) of the sodium channels: F 0.49; K_D = 10 nM.

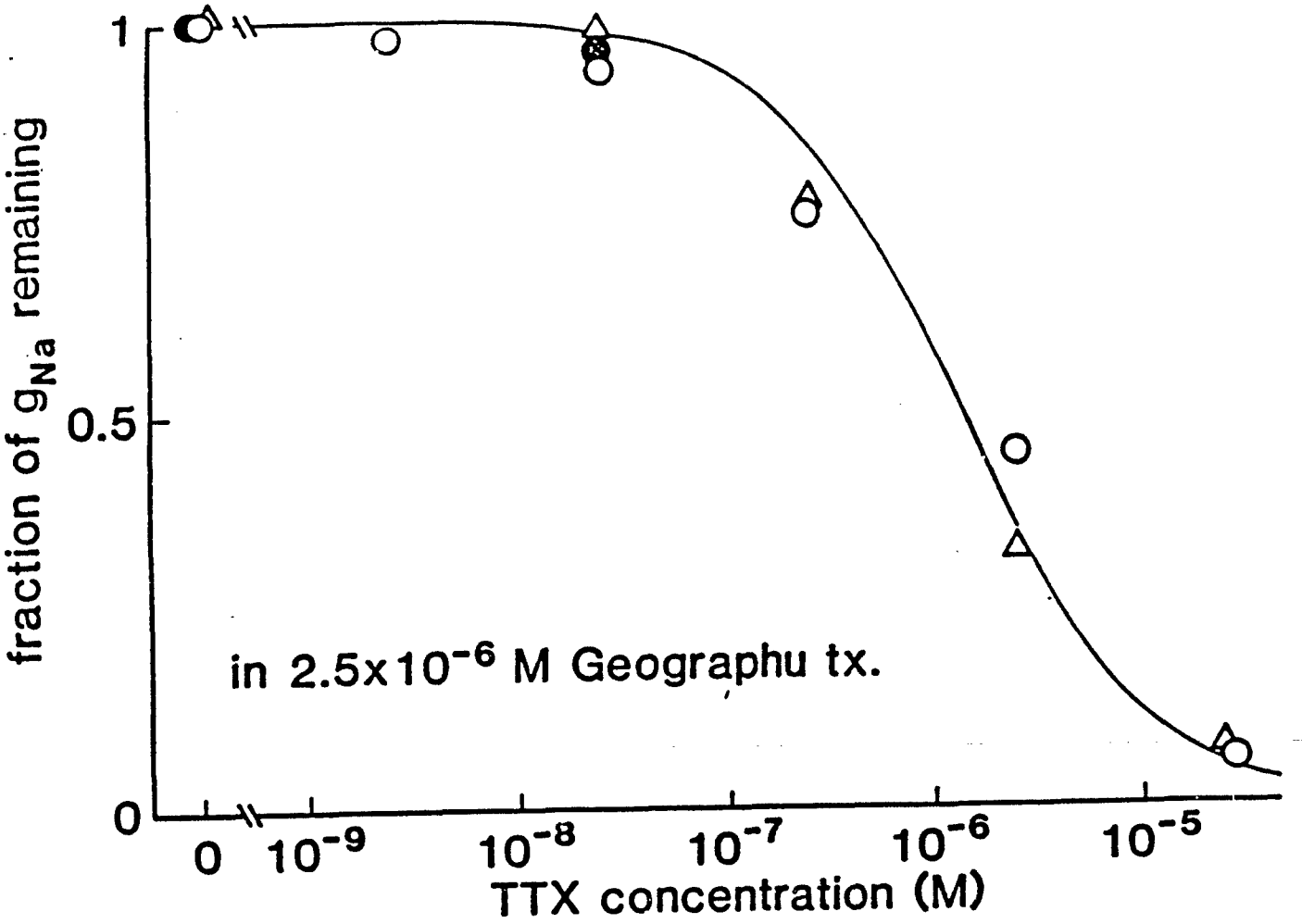

Figure 5. Concentration dependence of inhibition of sodium conductance by TTX in the presence of 2.5 μM GTX II. Myoballs were incubated in the presence of 2.5×10^{-6} M GTX II at room temperature (22 - 23°C) for 10 min before making a seal with a glass micropipet. After recording sodium currents in the presence of only GTX II, TTX concentration was increased cumulatively while the concentration of GTX II was kept constant and sodium currents were recorded. The different symbols represent different myoballs. The smooth curves in the figure represent a least squares fit assuming one-to-one, noncooperative binding of TTX to Na channels. K_D was 1.3 μM for TTX.

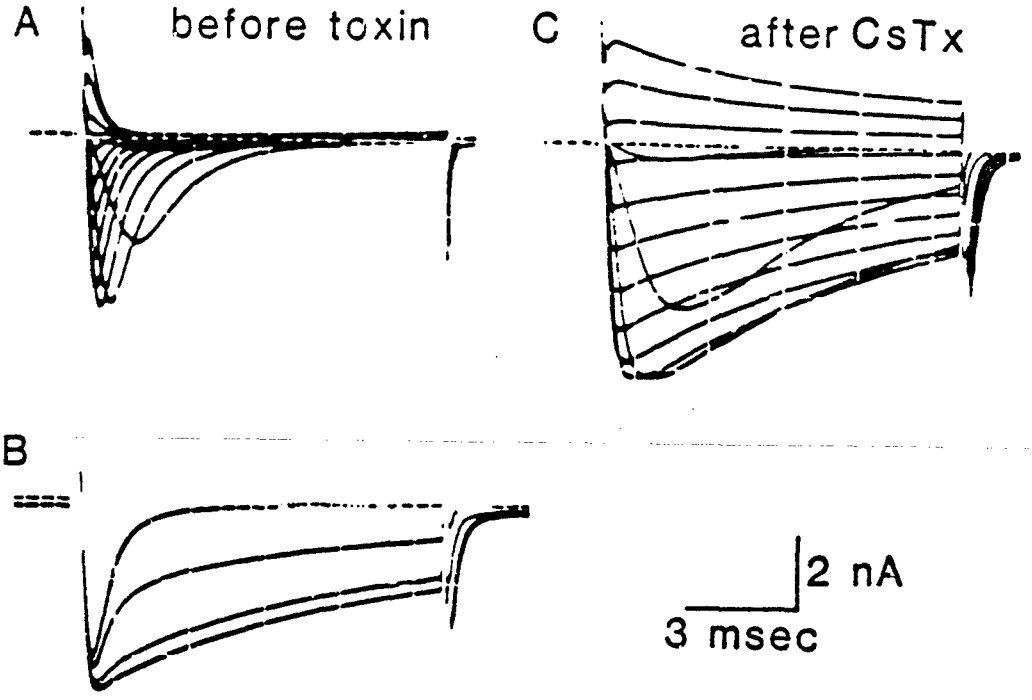

Figure 6. Effect of CsTx on the time course of sodium currents. **A.** A high resistance seal was formed on an N18 cell. After 20 min at a holding potential of -80 mV, the cell was hyperpolarized to -120 mV for 100 msec and depolarized for 10 msec to test potentials of -50 mV to +80 mV, in intervals of 10 mV, once per second to elicit the sodium currents illustrated. **B.** Eighteen µl of 4×10^{-6} M CsTx were added to the recording medium approximately 7 mm from the cell to give a final concentration in the recording bath of 1×10^{-7} M. Sodium currents were elicited every 30 sec by hyperpolarizing to -120 mV for 100 msec and depolarizing to +10 mV for 10 msec. Superimposed traces from a storage oscilloscope are shown. **C.** Six min after addition of CsTx, a family of sodium currents was recorded as in panel A.

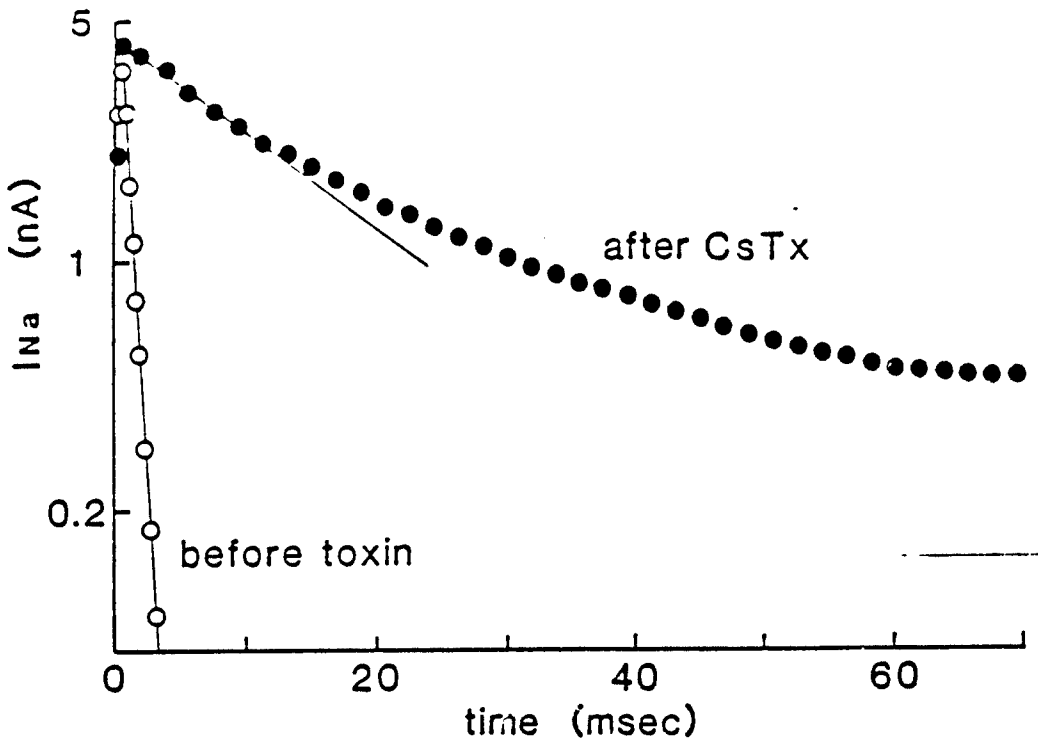

Figure 7. Time course of inactivation of the sodium current in the presence and absence of CsTx. A high resistance seal was formed on an N18 cell. After 20 min at a holding potential of -80 mV, a sodium current was recorded by hyperpolarizing to -120 mV for 100 msec and depolarizing to a test potential of +10 mV for 70 msec. CsTx was added at a final concentration of 1 x 10^{-7} M, the cell was incubated for 10 min at 37°C, and a sodium current was elicited by hyperpolarization to -120 mV for 100 msec and depolarization to +10 mV for 70 msec. The exponential decay of the currents is illustrated on semi-logarithmic coordinates. The limiting straight lines correspond to time constants of 0.7 and 15.8 msec, respectively.

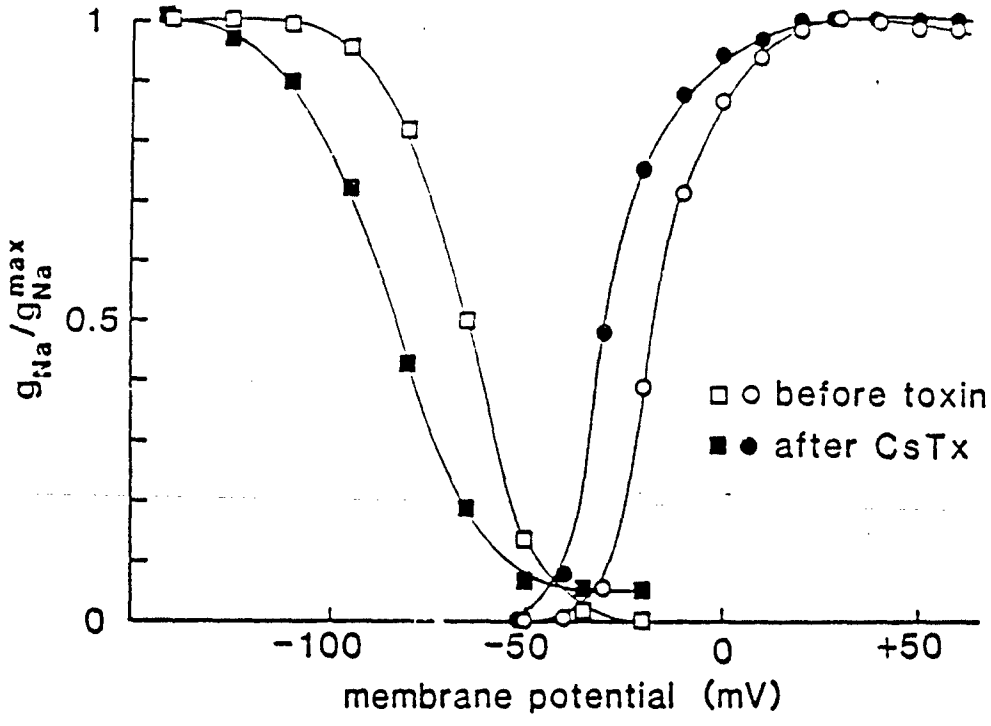

Figure 8. Effect of CsTx on the voltage-dependence of sodium channel activation and inactivation. Activation. Families of sodium currents were recorded in the presence and absence of 1 x 10^{-7} M CsTx as described in the legend to Fig. 6. Peak conductance values were calculated and plotted as the ratio of the measured value to g_{Na} observed in a pulse to +30 mV (before toxin,○; after toxin,●). Inactivation. N18 cells were hyperpolarized for 100 msec to the indicated membrane potentials and then sodium currents were elicited by a test pulse to +10 mV for 10 msec. Conductance values were calculated and plotted relative to the sodium conductance observed after a prepulse to -140 mV (before toxin,□; after toxin, ■).

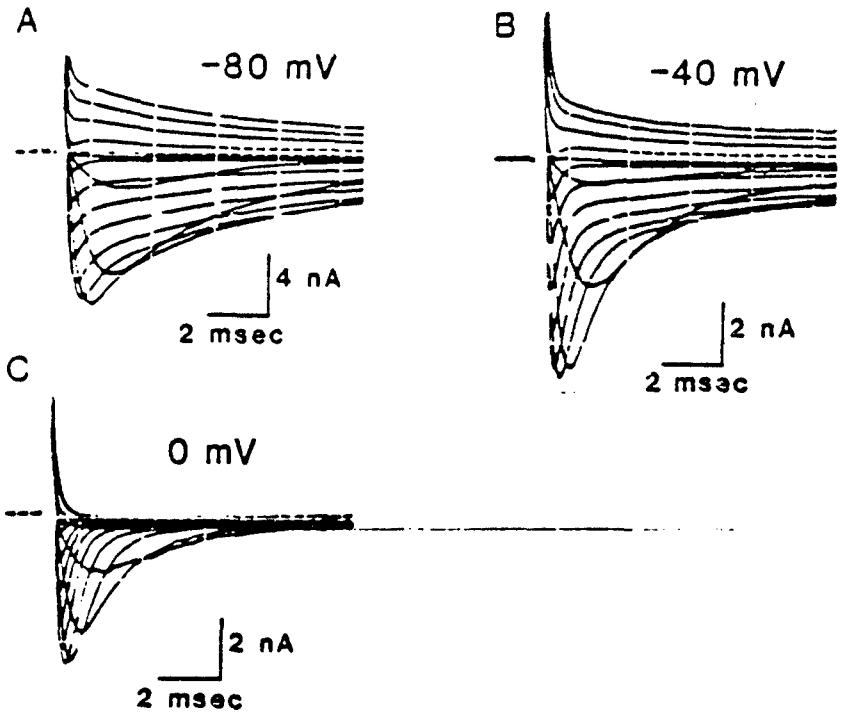

Figure 9. Voltage-dependence of CsTx action between -80 and 0 mV. **A.** N18 cells were incubated in the presence of 3 x 10^{-8} M CsTx at 37° C for 30 min. An individual cell at a holding potential of -80 mV was hyperpolarized to -120 mV for 200 msec and a family of sodium currents was elicited by 10 msec test pulses to potentials of -50 to +80 mV in intervals of 10 mV. **B.** The holding potential was changed to -40 mV for 5 min and a family of sodium currents was recorded as in A. **C.** The holding potential was then changed to 0 mV for 5 min and a family of sodium currents was recorded as in A.

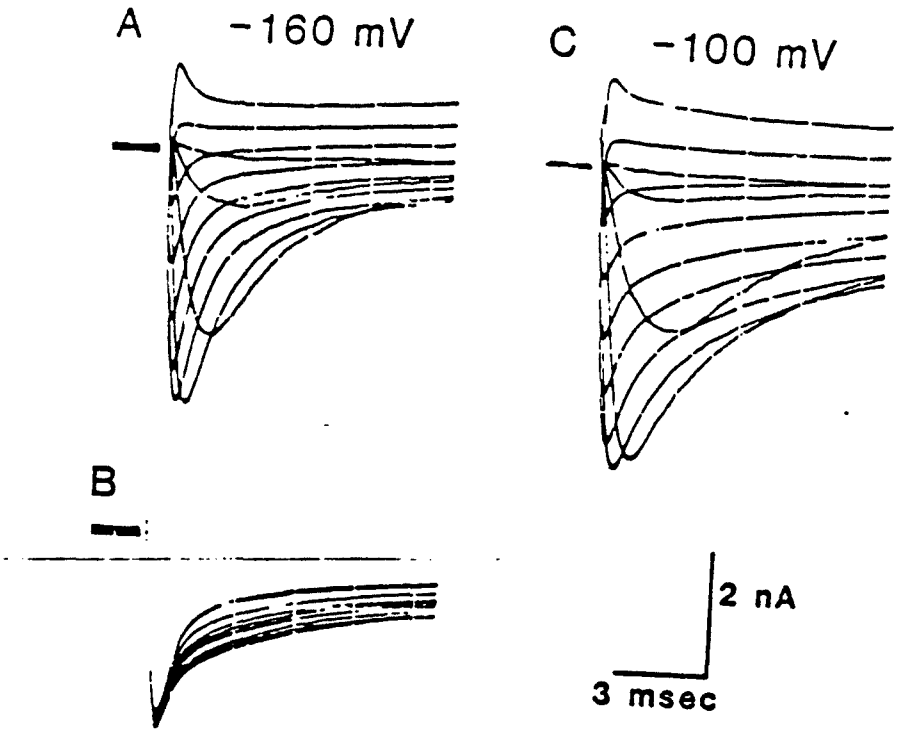

Figure 10. Voltage-dependence of CsTx action between -160 and -80 mV. **A.** N18 cells were incubated in the presence of 3 x 10^{-8} M CsTx at 37° C for 30 min. An individual cell at a holding potential of -80 mV was hyperpolarized to -160 mV for 10 min and a family of sodium currents was elicited by 10 msec test pulses to potentials of -50 mV to +60 mV in intervals of 10 mV. **B.** The holding potential was changed to -100 mV, sodium currents were elicited every 30 sec by 10 msec test pulses to +10 mV and the resulting traces were stored in a storage oscilloscope. Note the increase in slowly inactivated sodium current due to the depolarization. **C.** After 10 min at -100 mV, a family of sodium currents was elicited as in A except that the test pulse potentials ranged from -60 mV to +60 mV in intervals of 10 mV.

FIGURE 11A

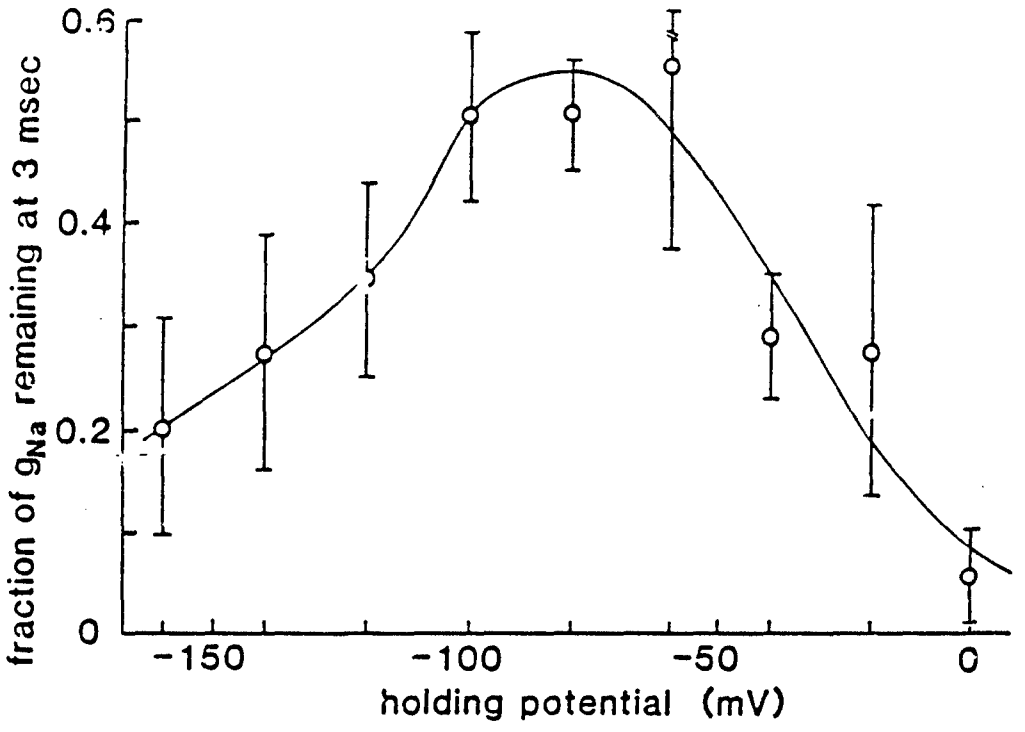

Figure 11. Voltage-dependence of the apparent K_D for CsTx. A. Sodium currents were recorded in the presence of 3 x 10-8 M CsTx as described in the legends to Figs. 9 and 10. The fraction of sodium conductance remaining 3 msec after the peak was measured and plotted as mean +/- S.D. for 3 to 9 cells at each membrane potential. The smooth curve connecting the data points was drawn by eye. B. The results of panel A were converted to values of apparent K_D assuming one-to-one binding of CsTx to sodium channels according to the relationship $K_D = [CsTx](F_g/[F_g-1])$, where F_g is the fraction of sodium conductance remaining 3 msec after the peak and F_g is the fraction of sodium conductance remaining 3 msec after the peak in the presence of a saturating concentration of CsTx (1 x 10-7 M) at a holding potential of -80 mV. The straight line illustrates the voltage dependence of binding of LqTx. The smooth curve is drawn by eye.

FIGURE 11B

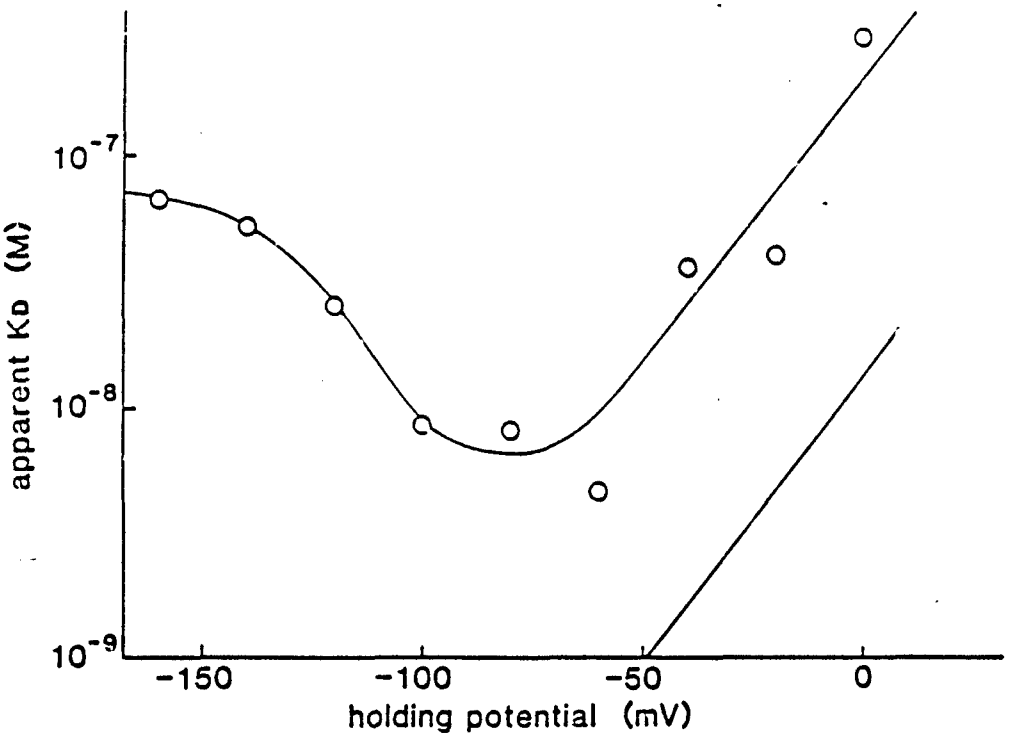

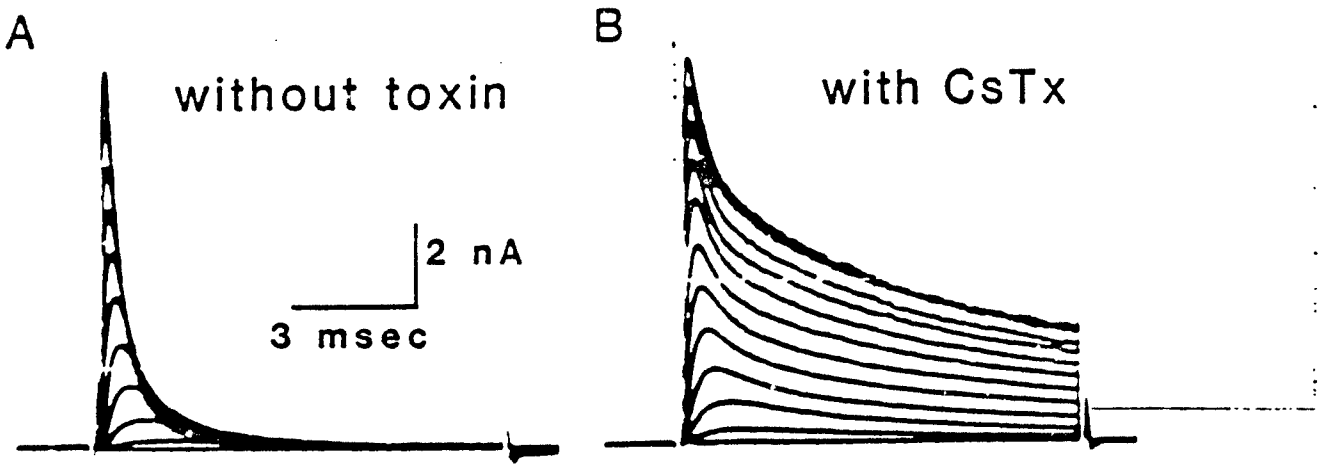

Figure 12. Effect of CsTx in sodium-free medium. **A.** N18 cells were incubated in choline-substituted, sodium-free recording medium in the absence of CsTx at 37° C for 30 min. The cells were maintained at a holding potential of -80 mV and families of outward sodium currents were recorded by hyperpolarizing to -120 mV for 100 msec followed by depolarizing to test potentials of -50 to +80 mV for 10 msec at intervals of one sec. **B.** The experiment in panel A was repeated after incubation for 30 min at 37°C the presence of 3×10^{-8} M CsTx. The outward sodium currents were completely blocked by addition of tetrodotoxin to a final concentration of 1×10^{-6} M.

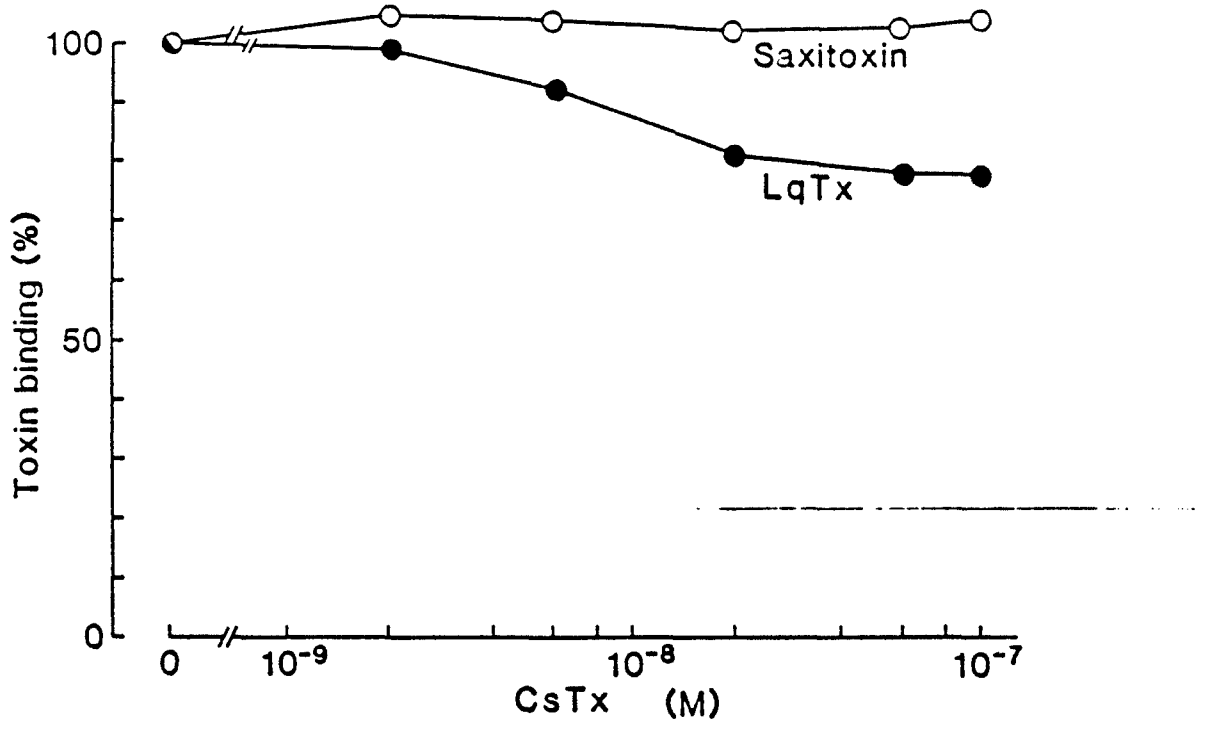

Figure 13. Effect of CsTx on binding of saxitoxin and Leiurus scorpion toxin to sodium channels. Specific binding of [3H]saxitoxin (○) and [^{125}I]Lqtx (●) to sodium channels in rat brain synaptosomes was measured in the presence of the indicated concentrations of CsTx.

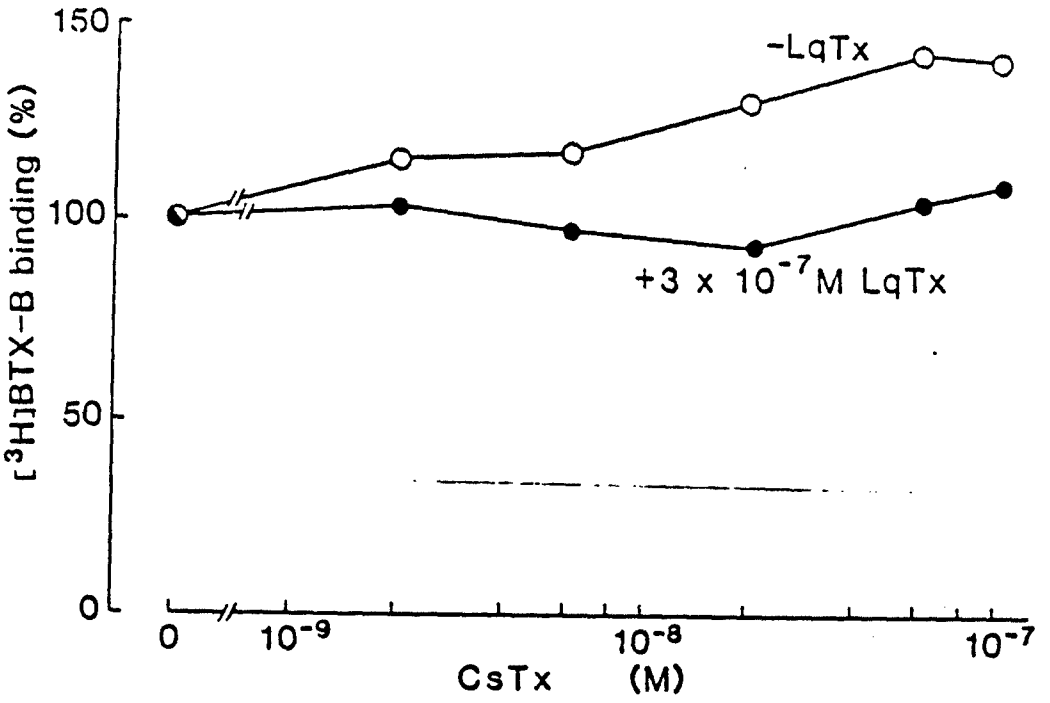

Figure 14. Effect of CsTx on binding of [^{3}H]BTX-B to sodium channels. Specific binding of [^{3}H]BTX-B to sodium channels in rat brain synaptosomes was measured without (○) or with (●) 3 x 10^{-7} M Lqtx in the presence of the indicated concentrations of CsTx.

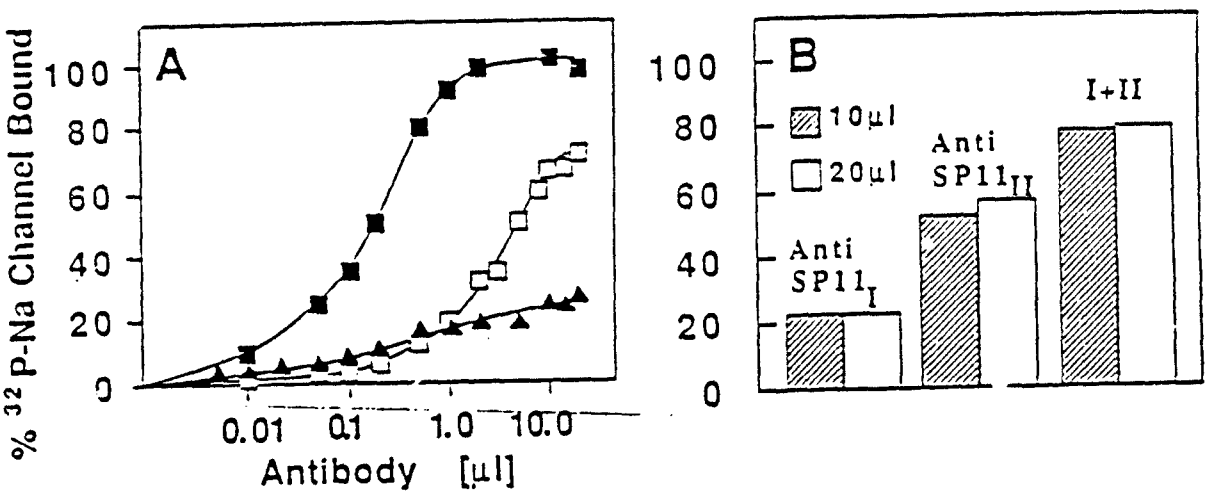

Figure 15. Additive immunoprecipitation of the R_I and R_{II} sodium channel subtypes. **A.** Purified, ^{32}P-labeled sodium channels (50 fmol) were immunoprecipitated with the indicated volumes of antibodies. Nonspecific immunoprecipitation (approximately 1% of total) was measured in the presence of 100 µM of the corresponding peptide and was subtracted from the data presented. Anti-SP1, closed square; anti-SP11$_I$, closed triangle; anti-SP11$_{II}$, open square. **B.** Additivity of immunoprecipitation of R_I and R_{II} from a different purified preparation of rat brain sodium channels by saturating volumes (10 µl or 20 µl as indicated) of anti-SP11$_I$ and anti-SP11$_{II}$ was measured as in panel A.

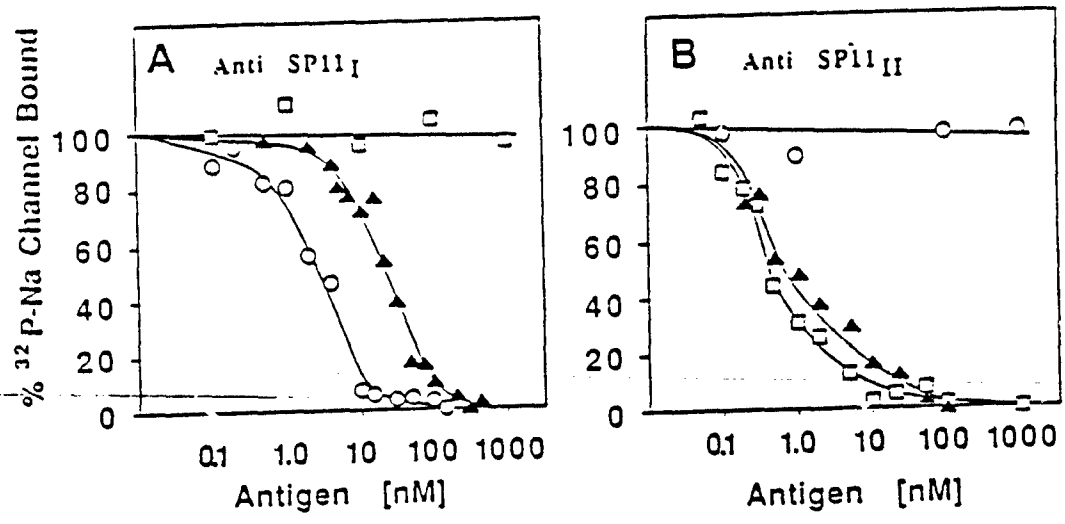

Figure 16. Specificity of immunoprecipitation by anti-SP11I and anti-SP11II. A. Fifty fmol of ^{32}P-labeled sodium channels were immunoprecipitated in the presence of the indicated concentrations of purified sodium channels (▲), $SP11_I$ (○), or $SP11_{II}$ (□). B. An identical experiment was carried out with anti-$SP11_{II}$.

Membrane fractions containing 100 fmol of saxitoxin binding sites were prepared and the R_I and R_{II} sodium channels were solubilized, immunoprecipitated with anti-SP1 (lanes 1), anti-$SP11_I$ (lanes 2), or anti-$SP11_{II}$ (lanes 3) antibodies, phosphorylated, and analyzed by $NaDodSO_4$-PAGE and autoradiography. **A.** Crude synaptosomal fraction (lysed P_3) from whole rat brain. **B.** Cerebral cortex. **C.** Hippocampus. **D.** Midbrain. **E.** Cerebellum. **F.** Medulla oblongata. **G.** Spinal cord. **H.** Optic nerve.

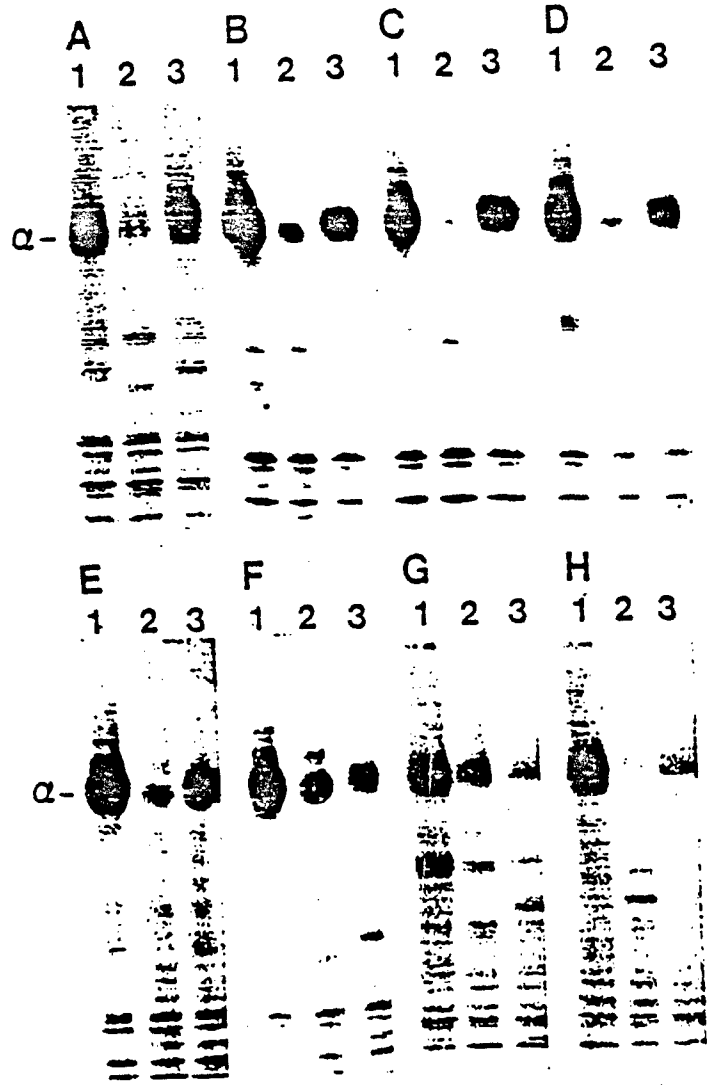

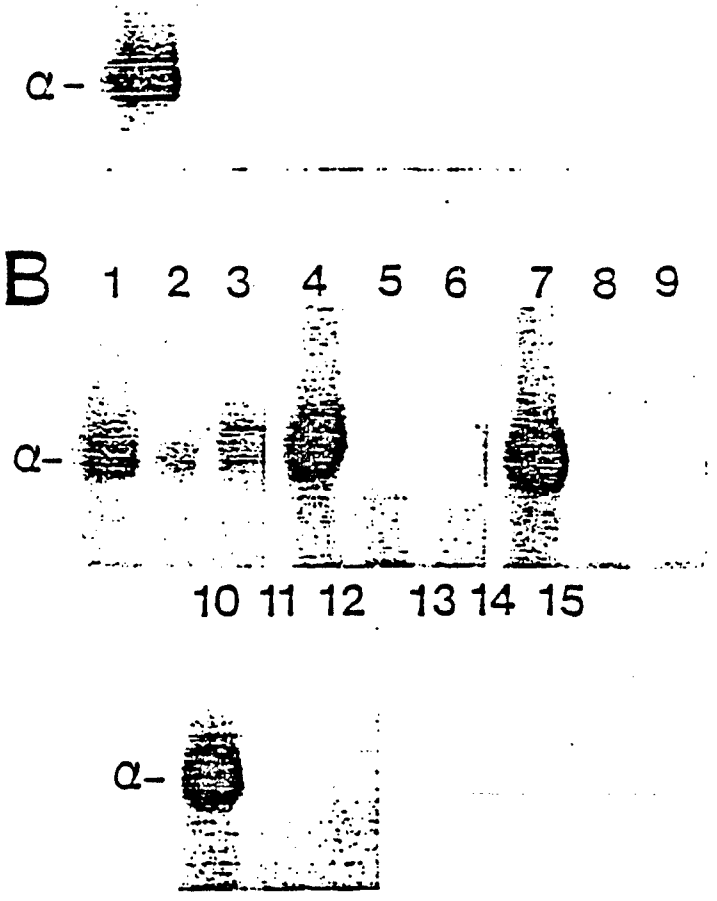

Figure 18. Expression of R_I and R_{II} in excitable tissues. **A.** Membrane fractions containing 100 fmol of saxitoxin binding sites were prepared from rat brain (lane 1), superior cervical ganglia (lane 2), skeletal muscle (lane 3), sciatic nerve (lane 4), and adrenal medulla (lane 5), and sodium channels were solubilized, immunoprecipitated with anti-SP1 antibodies, phosphorylated, and analyzed by $NaDodSO_4$-PAGE and autoradiography. **B.** Lanes 1-3. A membrane fraction was prepared from monkey (*Macaca nemestrina*) brain and sodium channels were solubilized, immunoprecipitated with anti-SP1 (lane 1), anti-$SP11_I$ (lane 2), or anti-$SP11_{II}$ (lane 3) antibodies, and analyzed by $NaDodSO_4$-PAGE and autoradiography. Lanes 4-6, chicken (*Gallus gallus*) brain; lanes 7-9, gecko (*Gecko gecko*) brain; lanes 10-12, frog (*Rana pipiens*) brain; and lanes 13-15, eel (*Electrophorus electricus*) brain.

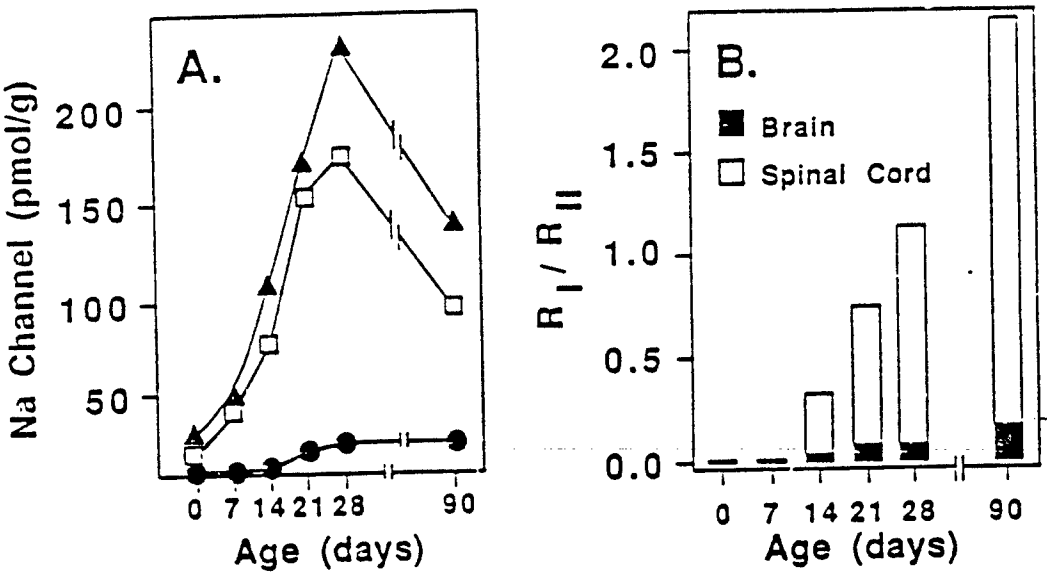

Figure 19. Developmental regulation of the expression of R_I and R_{II}. **A.** Brains were rapidly dissected from rats of the indicated ages, the cerebella were removed, and membrane fractions were isolated. Specific saxitoxin binding was measured at a saturating concentration (20 nM) (▲). Sodium channels were solubilized, immunoprecipitated with anti-$SP11_{II}$ (□) or anti-$SP11_{II}$ (●) antibodies, phosphorylated, and analyzed by $NaDodSO_4$-PAGE and autoradiography. The % R_I and R_{II} values were multiplied by the total number of saxitoxin binding sites to give pmol R_I and R_{II} per mg protein. **B.** A similar experiment was carried out with rat spinal cord and the data for both brain and spinal cord were plotted as the ratio of R_I/R_{II}.

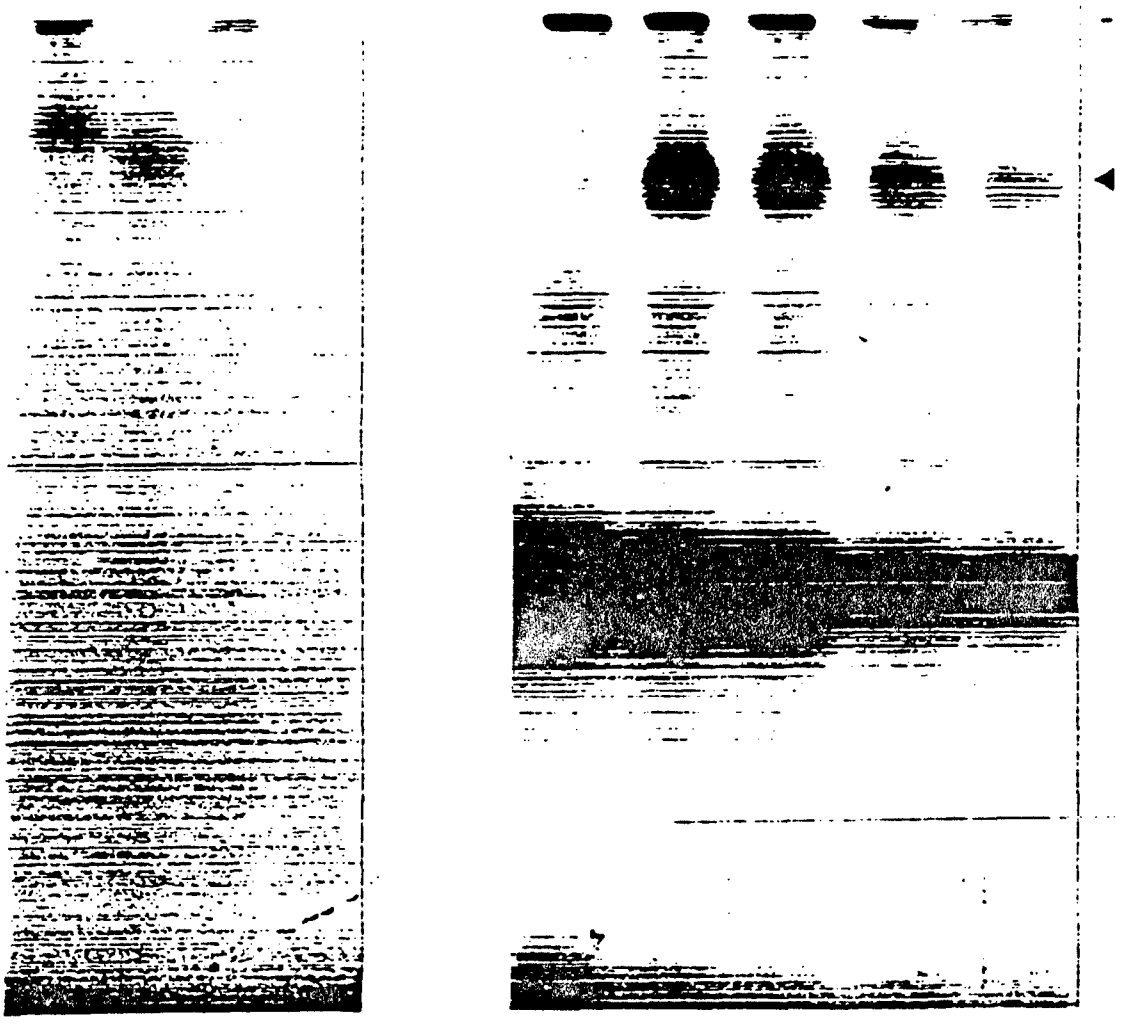

Figure 20. Photoaffinity affinity labeling of sodium channels by methylazidobenzimidyl Lqtx. **A.** Synaptosomes were incubated with [^{125}I]MAB-Lqtx in standard binding medium in the absence (lanes 1 and 2) or in the presence (lanes 3 and 4) of 200 nM native Lqtx for 10 min at 37° C. The samples were irradiated (λ_{max} = 354nm) for 20 min at 0° C. The labeled proteins were solubilized by boiling in SDS gel sample buffer in the absence (lanes 1 and 3) or presence (lanes 2 and 4) of 2-mercaptoethanol, resolved by SDS-PAGE, and visualized by autoradiography. **B.** Sodium channels were purified and reconstituted under conditions that restore binding of scorpion toxin. The reconstituted vesicles were incubated with [^{125}I]MAB-Lqtx in the presence of 200 nM native Lqtx (lane 1), 2 μM batrachotoxin plus 1 μM tetrodotoxin (lane 2), 1 μM tetrodotoxin (lane 3), 2 μM batrachotoxin (lane 4), or no additions (lane 5). The samples were irradiated for 20 min at 0° C and analyzed by SDS-PAGE and autoradiography. Arrowheads indicate the migration position of the free α subunit.

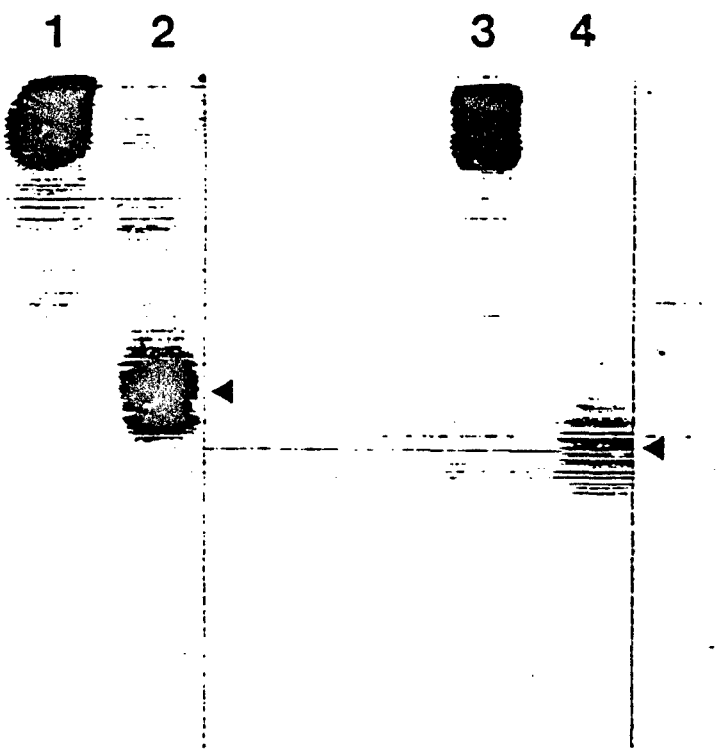

Figure 21. Cleavage of sodium channels covalently labeled with [^{125}I]Lqtx. Reconstituted sodium channels labeled by [^{125}I]ANB-Lqtx (lanes 1 and 2) or [^{125}I]MAB-Lqtx (lanes 3 and 4) and described in Figure 21 were solubilized in 1% Triton X-100. The photolabeled α subunit was purified by affinity chromotography on WGA-Sepharose. Samples were incubated for 20 min at 37°C with 15 µg/ml Staphylococcus aureaus protease V8. The untreated samples (lanes 1 and 3) and the protease cleaved samples (lanes 2 and 4) were then analyzed by SDS-PAGE and autoradiography. Arrowheads indicate the migration position of the 70 kDa fragment containing covalently attached [^{125}I]Lqtx.

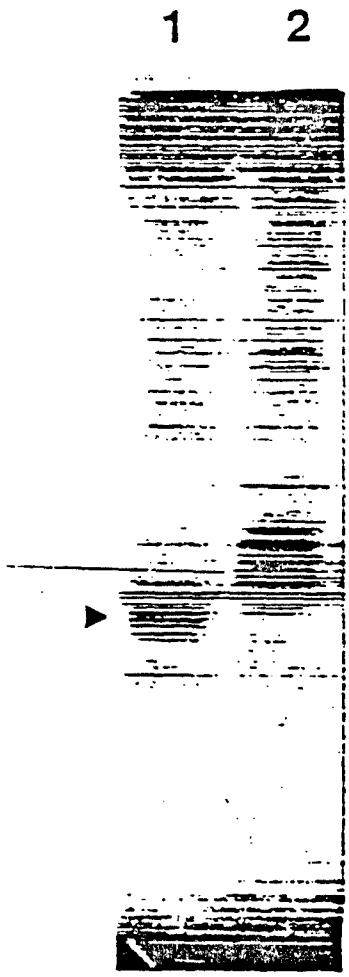

Figure 22. Cleavage of sialic acid from the 70 kDa [^{125}I]-LqTx-labeled sodium channels with neuraminidase. Reconstituted sodium channels were photoaffinity labeled with [^{125}I]ANB-LqTx, solubilized, and treated with Staphylococcus aureus V8 protease as described in Figure 21. The V8 fragment was then incubated for 60 min at 0° C with 0.5 μ neuraminidase (lane 1) or with no enzyme (lane 2). The samples were analyzed by SDS-PAGE and autoradiography. The arrowhead indicates the 50 kDa fragment observed after neuraminidase cleavage.

REFERENCES

Agnew, W. (1984) *Ann. Rev. Physiol.* **46**:517-530.

Albuquerque, E.X., Daly, J.W. (1976) In: *The Specificity and Action of Animal, Bacterial, and Plant Toxins*, P. Cuatrecasas, ed., Chapman and Hall, London, pp. 297-338.

Armstrong, C.M. (1981) *Physiol. Rev.* **61**:644-682.

Auld, V., Marshall, J., Goldin, A., Dowsett, A., Catterall, W., Davidson, N., Dunn, R. (1985) *J. Gen. Physiol.* **86**:10a.

Barchi, R.L., Weigele, J.B., Chalikian, D.M., Murphy, L.E. (1979) *Biochim. Biophys. Acta* **550**:59-76.

Barchi, R.L., Tanaka, J.D., Furman, R.E. (1984) *J. Cell. Biochem.* **26**:135-146.

Baumgold, J., Zimmerman, I., Bambrick, L. (1983) *Dev. Brain Res.* **9**:405-407.

Bergman, C., Dubois, J.M., Rojas, E., Rathmayer, W. (1976) *Biochim. Biophys. Acta* **455**:173-184.

Bolton, A.E., Hunter, W.M. (1973) *Biochem. J.* **133**:529-538.

Catterall, W.A. (1976) *Biochem. Biophys. Res. Commun.* **68**:136-142.

Catterall, W.A. (1977) *J. Biol. Chem.* **252**:8669-8676.

Catterall, W.A. (1979) *J. Gen. Physiol.* **74**:375-391.

Catterall, W.A. (1980) *Ann. Rev. Pharmacol. Toxicol.* **20**:15-43.

Catterall, W.A. (1984) *Science* **223**:653-661.

Catterall, W.A. (1985) in *Toxic Dinoflagellates*, eds. Anderson, White and Baden, Elsevier Science Publishing Comp., pp. 329-342.

Catterall, W.A. (1986) *Ann. Rev. Biochem.* **55**:953-985.

Catterall, W.A., Beress, L. (1978) *J. Biol. Chem.* **253**:7393-7396.

Catterall, W. A., Coppersmith, J. (1981) Mol. Pharmacol. 20:533-542.

Catterall, W.A., Morrow, C.S., Daly, J.W., Brown, G.B. (1981) *J. Biol. Chem.* **256**:8922-8927.

Catterall, W.A., Morrow, C.S., Hartshorne R.L. (1979) *J. Biol. Chem.* **254**:11379-11387.

Cohen, C.J., Bean, B.P., Colatsky, T.J., Tsien, R.W. (1981) *J. Gen. Physiol.* **78**:383-411.

Costa, M., Catterall, W.A. (1984) *J. Biol. Chem.* **259**:8210-8218.

Cruz, L.J., Gray, W.R., Olivera, B.M., Zeikus, R.D., Kerr, L., Yoshikami, D., Moczydlowski, E. (1985) *J. Biol. Chem.* **260**:9280-9288.

Endean R., Williams, H., Gyr, P., Surridge, J. (1976) *Toxicon* **14**:267-274.

Endean, R., Gyr, P., Surridge, J. (1977) *Toxicon* **15**:327-337.

Endean, R., Gyr, P., Surridge, J. (1979) *Toxicon* **17**:381-395.

Endean, R., Izatt, J., McColm, D. (1967) In: *Animal Toxins*. ed. Russell, F.E. & Saunders, P.R. Pergamon Press, Oxford, pp. 137-144.

Frelin, C., Vigne, P., Lazdunski, M. (1983) *J. Biol. Chem.* **258**:7256-7259.

Frelin, C., Vigne, P., Schweitz, H., Lazdunski, M. (1984) *Mol. Pharmacol.* **26**:70-74.

Fukuda J., Fischbach, G.D., Smith, T.G. (1976) *Dev. Biol.* **49**:412-424.

Goldin, A., Smith, T., Lubbert, H., Dowsett, A., Marshall, J., Auld, V., Downey, W., Fritz, L., Lester, H., Dunn, R., Catterall, W., Davidson, N. (1986) *Proc. Natl. Acad. Sci. USA* **83**:7503-7507.

Gonoi, T., Ashida, K., Feller, D., Schmidt, J., Fujiwara, M., Catterall, W.A. (1986) *Mol. Pharmacol.* **29**:347-354.

Gonoi, T., Hille, B. *J. Gen. Physiol.* **89**: in press.

Gonoi, T., Hille, B., Catterall, W.A.. (1984) *J. Neurosci.* **4**:2836-2842.

Gonoi, T., Sherman, S.J., Catterall, W.A. (1985) *J. Neurosci.* **5**:2559-2564.

Gray, W.R., Luque, A., Olivera, B.M. (1981) *J. Biol. Chem.* **256**:4734-4740.

Hahin, R., Wang, G.K., Strichartz, G.R., Schmidt, J., Shapiro, B.I. (1981) *Biophys. J.* **33**:124a.

Hamill, O.P., Marty, A., Neher, E., Sakmann, B., Sigworth, F.J. (1981) *Pflugers Arch.* **391**:85-100.

Harris, J.B., Marshall, M.W. (1973) *Nature* **243**:191-192.

Harris, J.B., Thesleff, S. (1971) *Acta. Physiol. Scand.* **83**:382-388.

Hunter, W.M., Greenwood, E.C. (1962) *Nature* **194**:495-496.

Kidokoro, Y., Heinemann, S., Schubert, D., Brandt, B.L., Klier, F.G. (1975) *Cold Spring Harbor Symp. Quant. Biol.* 40: 373-399.

Kobayashi, J., Nakamura, H., Hirata, Y., Ohizumi, Y. (1982) *Toxicon*, **20**:823-830.

Kobayashi, J., Nakamura, H., Hirata, Y., Ohizumi, Y. (1982) *Biochem. Biophys. Res. Commun.* **105**:1389-1395.

Kobayashi, J., Nakamura, H., Ohizumi, Y. (1981) *Br. J. Pharmacol.* **73**:583-585.

Kobayashi, M., Wu, C.H., Yoshii, M., Narahashi, T., Nakamura, H., Kobayashi, J., Ohizumi, Y. (1986) *Pflugers Archiv.* 241-243.

Koppenhofer, E., Schmidt, H. (1968) *Pflugers Archiv.* **303**:150-161.

Kryshtal, O.A., Osipchuk, Y.V., Kozlovskaya E.P. (1982) *Neurophys.* **14**:303-309.

Lawrence, J.C., Catterall, W.A. (1981) *J. Biol. Chem.* **256**:6223-6229.

Lombet, A., Kazazoglou, T., Delpont, E., Renaud, J., Lazdunski, M. (1984) *Biochem. Biophys. Res. Commun.* **110**:894-901.

Maizel, J.V. (1971) *Meth. Virol.* **51**:179-224.

Mandell, G., Cooperman, S., Montminy, M., Barchi, R., Brehm, P., Goodman, R. (1986) *Biophys. J.* **49**:380a.

Merrifield, R.B. (1963) *J. Amer. Chem. Soc.* **85**:2149-2154.

Minoshima, S., Kobayashi, M., Nakamura, H., Kobayashi, J. Ogura, A., Takahashi, M., Ohizumi, Y. (1984) *Japan J. Pharmacol.* **36**:192p.

Moczydlowski, E., Olivera, B.M., Gray, W.R., Strichartz, G.R. (1986) *Proc. Natl. Acad. Sci. USA* **83**:5321-5325.

Mozhayeva, G.N., Naumov, A.P., Nosyreva, E.D., Grishin E.V. (1980) *Biochim. . Biophys. Acta* **597**:587-602.

Nakamura. H., Kobayashi, J., Ohizumi, Y., Hirata, Y. (1983) *Experientia* **39**:590-591.

Noda, M., Shimizu, S., Tanabe, T., Takai, T., Kayano, T., Ikeda, T., Takahashi, H., Nakayama, H., Kanaoka, Y., Minamino, N., Kangawa, K., Matsuo, H., Raftery, M., Hirose, T., Inayama, S., Hayashida, H., Miyata, T., Numa, S. (1984) *Nature* **312**:121-127.

Noda, M., Ikeda, T., Kayano, T., Suzuki, H., Takeshima, H., Kurasaki, M., Takahashi, H., Numa, S. (1986) *Nature* **320**:188-192.

Ohizumi, Y., Nakamura, H., Kobayashi, J. (1986a) *Eur. J. Pharmacol.* **120**:245-248.

Ohizumi, Y., Nakamura, H., Kabayashi, J., Catterall, W.A. (1986b) *J. Biol. Chem.* **261**:6149-6152.

Olivera, B.M., McIntosh, M., Cruz, L.J., Luque, F.A., Gray, W.R. (1984) *Biochemistry* **23**:5087-5090.

Olivera, B.M., Gray, W.R., Zeikus, R., McIntosh, J.M., Varga, J., Rivier, J., de Santos, V., Cruz, L.J.. (1985) *Science* **230**:1338-1343.

Olmsted, J. B. (1981) *J. Biol. Chem.* **256**:11955-11957.

Orth, D.N. (1979) in *Methods Hormone Radioimmunoassay*, eds. Jaffe, B.M. & Behrman, H.R., (Academic Press, New York, NY), pp. 245-284.

Pappone, P.A. (1980) *J. Physiol. (Lond.)* **306**:377-410.

Reuter, H. (1979) *Ann. Rev. Physiol.* **41**:413-424.

Ritchie, J.M., Rogart, R.B. (1977) *Rev. Physiol. Biochem. Pharmacol.* **79**:1-49.

Sastre, A., Podleski, T.R. (1976) *Proc. Natl. Acad. Sci. USA* **73**:1355-1359.

Sato, S., Nakamura, H., Ohizumi, Y., Kobayashi, J., Hirata Y. (1983) *FEBS Lett.* **155**:277-280.

Schmidt, J., Rossie, S., Catterall, W. (1985) *Proc. Natl. Acad. Sci. USA* **82**:4847-4851.

Sherman S.J., Lawrence, J.C., Messner, D.J., Jacoby, K., Catterall, W.A. (1983) *J. Biol. Chem.* **258**:2488-2495.

Stallcup, W.B., Cohn, M. (1976) *Exp. Cell Res.* **98**:277-284.

Sumikawa, K., Parker, I., Miledi, R. (1984) *Proc. Natl. Acad. Sci. USA* **81**:7994-7998.

Unsworth, B., Hafemann, D. (1975) *J. Neurochem.* **24**:261-270.

Warashina, A., Fugita, S. (1983) *J. Gen. Physiol.* **81**:305-323.

Weiss, R.E., Horn, R. (1986) *Science*, in press.

Wollner, D., Catterall, W.A. (1985) *Brain Res.* **331**:145-149.

Yanagawa, Y., Abe, T., Satake, M. (1986) *Neurosci. Lett.* **64**:7-12.

DISTRIBUTION LIST

5 copies	Commander U.S. Army Medical Research Institute of Infectious Diseases ATTN: SGRD-UIZ-M Fort Detrick, Frederick, MD 21701-5011
1 copy	Commander U.S. Army Medical Research and Development Center ATTN: SGRD-RMI-S Fort Detrick, Frederick, MD 21701-5012
12 copies	Defense Technical Information Center (DTIC) ATTN: DTIC-DDAC Cameron Station Alexandria, VA 22304-6145
1 copy	Dean School of Medicine Uniformed Services University of the Health Sciences 4301 Jones Bridge Road Bethesda, MD 20814-4799
1 copy	Commandant Academy of Health Sciences, U.S. Army ATTN: AHS-CDM Fort Sam Houston, TX 78234-6100

END

DATE

FILMED

5-88

DTIC